Cold sensitivity of the SARS-CoV-2 spike ectodomain

Robert J Edwards[1,2‡,*], Katayoun Mansouri[1,‡], Victoria Stalls[1,‡], Kartik Manne[1, ‡], Brian Watts[1], Rob Parks[1], Katarzyna Janowska[1], Sophie M. C. Gobeil[1], Megan Kopp[1], Dapeng Li[1], Xiaozhi Lu[1], Zekun Mu[1], Margaret Deyton[1], Thomas H Oguin III[1], Jordan Sprenz[1], Wilton Williams[1,2], Kevin Saunders[1,3], David Montefiori[1,3], Gregory D. Sempowski[1], Rory Henderson[1,2], Munir Alam[1,2], Barton F. Haynes[1,2], Priyamvada Acharya[1,3,*]

Affiliations:
[1] Duke Human Vaccine Institute, Durham NC 27710, USA
[2] Duke University, Department of Medicine, Durham NC 27710, USA
[3] Duke University, Department of Surgery, Durham NC 27710, USA
[4] Duke University, Department of Immunology, Durham NC 27710, USA
‡These authors contributed equally.
*To whom correspondence should be addressed

Correspondence to: Robert J Edwards (rj.edwards@duke.edu) and Priyamvada Acharya (priyamvada.acharya@duke.edu)

Abstract

The SARS-CoV-2 spike (S) protein, a primary target for COVID-19 vaccine development, presents its Receptor Binding Domain in two conformations: receptor-accessible “up” or receptor-inaccessible “down” conformations. Here, we report that the commonly used stabilized S ectodomain construct "2P" is sensitive to cold temperature, and that this cold sensitivity is resolved in a “down” state stabilized spike. Our results will impact structural, functional and vaccine studies that use the SARS-CoV-2 S ectodomain.

44 The spike (S) protein of SARS-CoV-2 mediates receptor binding and cell entry and is a
45 key target for vaccine development efforts. Stabilized S ectodomain constructs have been
46 developed that mimic the native spike, bind ACE-2 receptor [1,2], and present epitopes for
47 neutralizing antibodies on their surface [3-6]. The "2P" S-ectodomain construct examined here
48 incorporates residues 1-1208 of the SARS-CoV-2 spike, with two proline mutations in C-terminal
49 S2 domain designed to stabilize the pre-fusion spike conformation, a C-terminal foldon
50 trimerization motif, and a mutation that abrogates the furin cleavage site [1] (Figure 1a). This and
51 similar constructs are being widely used for structural biology and vaccine studies [1-3,7,8]. Purified
52 S ectodomain proteins [9] are assessed for quality control by SDS-PAGE, size exclusion
53 chromatography (SEC), differential scanning fluorimetry (DSF) [10], and negative stain electron
54 microscopy (NSEM). NSEM has proved especially important because it reveals the three-
55 dimensional structural integrity of individual molecules, allowing us to discriminate between
56 preparations that looked similar by bulk methods such as SDS-PAGE and SEC (Extended Data
57 Figure 1). The observed variability in the spike fraction between preparations suggests a fragile
58 S ectodomain, and measures to overcome the issue have been previously reported [11,12]. Here
59 we link the apparent fragility of spike ectodomain 2P to its rapid denaturation upon storage at 4
60 °C (Figure 1 b-e).

61 We followed the structural, biophysical and antigenic features of the S ectodomain
62 stored under different temperatures conditions (Figure 1, Extended Data Figures 2-6). The 2P
63 spike was produced in 293F cells at 37 °C and the purification was performed at room
64 temperature and completed within 6-8 hours (Supplementary Figure 1a-c) . Representative
65 NSEM micrographs obtained of the 2P spike incubated at different temperatures and shown
66 (Figure 1b-d, Supplementary Figure 1d-e) , and results summarized in Figure 1e. Freshly
67 prepared spike samples assessed on the same day they were purified showed 75% well-formed
68 spikes on average (Fig 1b,e); this fraction slightly decreased to 64% after one cycle of

69 freeze/thaw and to 59% by storage at room temperature (22 ºC) for 5–7 days (Supplementary
70 Figure 1d,e); and it was substantially reduced to 5% after storage at 4 ºC for 5–7 days (Fig
71 1c,e). In contrast, after 1-week storage at 37 °C, we observed 83% well-formed spike.
72 Furthermore, well-formed spike could be recovered after the spike was stored at 4 °C for a week
73 with a 3-hour incubation at 37 °C to ~75% (Figure 1d,e); no further improvement was observed
74 after longer incubations at 37 °C (Figure 1e) which actually led to slight aggregation
75 (Supplemental Figure 1e). SDS-PAGE analysis (Supplementary Figure 1) of 2P spike samples
76 stored at different temperatures does not indicate any appreciable degradation of the spike,
77 although we do observe evidence of higher molecular weight species in spike stored at 37 °C
78 for a week (Supplemental Figure 1). Similar to our NSEM results, we also see substantial
79 differences in the quality and dispersion of protein in cryo-EM grids depending on the
80 temperature the specimen was stored (Extended Data Figure 6). In summary, these data show
81 that the 2P spike denatured upon storage for at 4 °C for a week, and this denaturation could be
82 at least partially reversed by incubating the sample at 37 °C following cold-storage.

83 The S ectodomain was reported to exhibit conformational changes in response to pH[12],
84 so we asked whether the spike denaturation observed was due to temperature-dependent pH
85 changes at 4 °C in the Tris pH 8.0 buffer we used[13] . A Tris buffer solution that measures pH 8.0
86 at 25 °C would measure ~pH 8.6 at 4 °C. We performed SEC purification of a 2P spike
87 preparation into MOPS buffer pH 7.4. MOPS has a smaller temperature dependence compared
88 to Tris[13], and is expected to change only slightly to pH 7.42 at 4 °C . Cold-storage at pH 7.42
89 (MOPS buffer) reduced the spike fraction to 4%, similar to the average of 5% for cold-storage in
90 Tris buffer (Figure 1e). Thus, the primary cause of spike denaturation appears to be the
91 temperature change and not the pH shift within this range. We also tested the temperature
92 effect at acidic pH and found that incubating the spike at 4 °C in MES, pH 6 buffer reduced but
93 did not eliminate the cold-sensitivity (Fig 1e).

94 We next examined whether the observed cold sensitivity is a property of the bulk protein
95 in solution, rather than an artifact of the NSEM sample preparation. First, we used a rapid DSF
96 assay[10] that measures changes in the intrinsic fluorescence of the protein as a thermal ramp is
97 applied. The changes in fluorescence signal indicate transitions in the folding state of a protein,
98 the temperature at which a transition occurs is called the inflection temperature (Ti). Distinct
99 profile shifts were observed for spike samples stored at different temperatures, with Ti shifted
100 toward lower temperatures for spike samples stored at 4 °C, indicating lower protein stability,
101 compared to when the spike was stored at 22 °C or 37 °C (Figures 1f). Next, we measured
102 melting temperatures (T_m) using differential scanning calorimetry (DSC) (Figure 1g and
103 Extended Data Figure 3): after one-week storage at 37 °C, the spike sample featured an
104 asymmetric unfolding transition with T_m of 65.5 °C. After one-week storage at 22 °C, we
105 observed a second low-T_m transition at 48.2 °C. After one-week storage at 4°C, we observed a
106 similar two-peak profile with a markedly more pronounced low-T_m transition (T_m = 48.4 °C).
107 Upon returning the 4 °C sample to 37 °C for 3 hours prior to analysis, we observed an amplitude
108 reduction of the low-T_m transition (T_m = 49.2 °C) and a corresponding amplitude increase in the
109 high-T_m transition (T_m = 66.0 °C). Thus, the DSC results confirm that storage at 4 °C
110 destabilizes the spike compared to samples stored at 22 °C or 37 °C, and that returning the
111 destabilized spike to 37 °C for 3 hours substantially restores its stability, although the presence
112 of the low-Tm peak suggests that the recovery is partial.

113 We next tested the effects of cold-induced spike instability on antibody and receptor
114 binding by SPR and ELISA (Figures 1h and Extended Data Figures 4-5, Supplementary Figure
115 2). We found that spike stored at 4 °C showed higher binding to antibody CR3022 (Figure 1h,
116 Extended Data Figure 4, Supplementary Figure 2) and the receptor ACE-2 (Extended Data
117 Figure 4), which both require an “up” RBD conformation for stable binding[1,9,12]. In contrast, cold-
118 storage reduced binding to antibody 2G12 (Figure 1h, Extended Data Figure 4, Supplementary

119 Figure 2), which recognizes a quaternary glycan epitope in the S2 subunit[14] indicating loss of
120 quaternary structure during cold storage. We also tested two antibodies isolated from a COVID-
121 19 convalescent donor (Supplementary Figures 4-5), with epitopes mapped to the ACE-2
122 binding site (AB712199) and to the S2 region of the spike (AB511584) (Supplementary Figure
123 4). Both antibodies showed different binding profiles depending on the temperature at which the
124 spike was stored, highlighting the importance of accounting for this cold-sensitive behavior of
125 the S ectodomain for obtaining consistent results in serology assays when using the 2P spike or
126 similar constructs. We next tested CR3022 and 2G12 binding to freshly prepared 2P spike
127 sample and compared it to a sample that was flash frozen in liquid N2, stored in single-use
128 aliquots at -80 °C and thawed by incubating at 37 °C Supplementary Figure 3). We found that
129 freeze-thaw increased CR3022 binding to the 2P spike relative to the fresh sample, although
130 incubation at 37 °C of the thawed sample for 20 min reduced binding close to the levels
131 observed in the fresh sample. Based on these data, in order to obtain consistent results in
132 binding studies, we recommend flash-freezing spike samples in single use aliquots, thawing at
133 37 °C followed by a brief (~20 min) incubation at 37 °C before using the 2P spike in binding
134 studies.

135 These results suggested that cold-induced denaturation of spike was associated with
136 increased RBD-exposure of the S ectodomain, and we thus asked whether a “down” state
137 stabilized S ectodomain might be resistant to cold-induced denaturation (Figure 2). We included
138 in this analysis a variant that combined the recently described rS2d[9] and HexaPro mutations[11]
139 (Figure 2a,b). This new variant, named rS2d-HexaPro, showed the highest production yields of
140 the all-RBD-down spike constructs (Figure 2c). Similar to the rS2d construct[9], rS2d-Hexapro
141 was shown by NSEM to be 100 % in a 3-RBD-down conformation (Figure 2d,e, Extended Data
142 Figure 7 and Supplementary Movie 1). Both HexaPro and rS2d-HexaPro appeared more
143 resistant to cold-induced denaturation (Figure 2f) than the 2P spike (Figure 1e), with rS2d-

144 HexaPro showing a higher intact spike percentage than HexaPro (Figure 2f). The rS2d
145 mutations (D985C, S383C) introduce an inter-protomer disulfide bond between the RBD and the
146 S2 domain, which we suggest stabilizes the spike and prevents its cold-induced denaturation.
147 An independent study also reported that the 985C-383C disulfide bond, as well as an introduced
148 disulfide between residues 987 and 413, prevented denaturation of the spike when stored at 4
149 °C[15]. These data suggest that inter-promoter disulfide linkages may be a general strategy for
150 stabilization of the 2P spike ectodomain and preventing its cold-induced denaturation. We also
151 included two glycan-deleted mutants, 2P-N165A and 2P-N234A[16], that favor the RBD "up" or
152 "down" conformation, respectively (Figure 2f), and both mutants showed substantial reduction of
153 spike percentage after incubation at 4 °C (Figure 2f), Thermostability and binding studies
154 (Figures 2g,h) further confirmed that both HexaPro and rS2d-HexaPro were more resistant to
155 cold destabilization compared to the 2P version (Figure 1). ACE-2 binding to rS2d-HexaPro was
156 substantially reduced for samples stored at all temperatures, as expected for a spike construct
157 fixed in an RBD-down conformation. Similarly, binding to 2G12 remained same for the rS2d-
158 HexaPro construct irrespective of the storage temperature of the 2P spike (Figure 1h), showing
159 that the rS2d-Hexapro structure remains unperturbed upon 4 °C storage. For HexaPro, binding
160 to ACE-2 was higher and 2G12 binding was reduced with 4 °C -stored protein compared to 37
161 °C-stored samples, showing that the HexaPro structure remained susceptible to perturbation at
162 lower temperatures.

163 Overall, our results demonstrate the cold sensitivity of the furin-cleavage deficient
164 SARS-CoV-2 ectodomain, and its impact on antibody and receptor binding. We have also
165 shown that this cold destabilization is substantially reduced in the HexaPro spike and further
166 reduced by stabilization of the S ectodomain in a disulfide-locked "down" position.

167 **Acknowledgements**

168 This work was supported by NIH NIAID extramural project grants R01 AI145687 (P.A.), and
169 AI058607 (G.S.), funding from the Department of Defense HR0011-17-2-0069 (G.S.) and a
170 contract from the State of North Carolina Pandemic Recovery Office through funds from the
171 Coronavirus Aid, Relief, and Economic Security (CARES) Act (B.F.H.). This work utilized the
172 DSC platform supported by the Duke Consortia for HIV/AIDS Vaccine Development (CHAVD)
173 and the Titan Krios microscope in the Shared Materials and Instrumentation Facility at Duke
174 University. The following reagent was deposited by the Centers for Disease Control and
175 Prevention and obtained through BEI Resources, NIAID, NIH: SARS-Related Coronavirus 2,
176 Isolate USA-WA1/2020, NR-52281. MN and PRNT assays were performed in the Virology Unit
177 of the Duke Regional Biocontainment Laboratory, which received partial support for construction
178 from the National Institutes of Health, National Institute of Allergy and Infectious Diseases (UC6-
179 AI058607).

180 **Author contributions**

181 R.J.E., K.Mansouri., V.S. and P.A. discovered the effect of storage temperature on spike
182 stability. R.J.E. led NSEM studies and established quantitative metrics for spike QC. K.Mansouri
183 collected NSEM data and performed analyses. V.S. purified proteins and performed
184 thermostability measurements. K.Manne purified proteins, performed SPR assays, prepared
185 samples for NSEM, Tycho, ELISA, SPR and DSC measurements, and coordinated the study
186 between the different research teams. B.W. performed DSC measurements. R.P., M.D. J.S. and
187 W.W. performed ELISA assays. D.L., X.L., K.S. and G.S. isolated antibodies from convalescent
188 patient. S.G. and K. J. purified proteins and performed thermostability assays. M.F.K purified
189 proteins. Z.M. performed binding measurements. R.H. initiated the DSC experiments and
190 provided the rS2d, 2P-N234A and 2P-N165A constructs prior to publication. M.A. supervised
191 the DSC experiments. B.F.H. supervised ELISA experiments and antibody isolation. P.A.

192 oversaw and led the study, and co-wrote the paper with R.J.E. and V.S. All authors reviewed
193 and commented on the manuscript.
194

195 **Methods**

196 *Protein expression and purification*

197 SARS-CoV-2 ectodomain constructs were produced and purified [1,11] as follows. A gene
198 encoding residues 1−1208 of the SARS-CoV-2 S (GenBank: MN908947) with proline
199 substitutions at residues 986 and 987, a "GSAS" substitution at the furin cleavage site (residues
200 682–685), a C-terminal T4 fibritin trimerization motif, an HRV3C protease cleavage site, a
201 TwinStrepTag and an 8XHisTag was synthesized and cloned into the mammalian expression
202 vector pαH. Plasmids were transiently transfected into either FreeStyle-293F cells using
203 Turbo293 (SpeedBiosystems). Cells were grown in a 37 °C incubator with 9 % CO2 and 120
204 rpm rotary motion. Protein was purified on the sixth day post-transfection from filtered
205 supernatant using StrepTactin resin (IBA), followed by SEC purification using a Superose 6
206 10/300 Increase column in nCoV buffer (2mM Tris, pH 8.0, 200 mM NaCl, 0.02% sodium azide).
207 rS2d-Hexapro was also grown in CHO cells. Plasmids were transiently transfected into CHO
208 cells using ExpiFectamine CHO Transfection Kit (ThermoFisher), and protein was purified one
209 the sixth day post-transfection. All protein purification steps including Strep tag purification and
210 SEC were performed at room temperature. The spikes were purified the same day that the cells
211 are harvested and the purification is completed 6-8 hours. The purified protein is flash frozen
212 and stored in -80 °C in single-use aliquots. Each aliquot is thawed and briefly incubated (~20
213 min) at 37 °C before use.

214 Antibodies were produced in Expi293 cells and purified by Protein A affinity. For ACE-2
215 constructs, the ACE-2 C-terminus was fused with either the human or mouse Fc region
216 including C-terminal 6X His-tag on the Fc domain. ACE-2 with human Fc tag was purified by
217 Protein A affinity chromatography, and ACE-2 with mouse F_C tag was purified by Ni-NTA
218 chromatography.

219

220 *Negative-stain electron microscopy*

221 Spike samples were pre-incubated (stored) for specified times in nCoV buffer at 4, 22 or 37 °C,
222 then moved to room temperature for preparation of NSEM grids, which was complete in less
223 than 5 min. Samples were diluted to 100 µg/ml with room-temperature buffer containing 20 mM
224 HEPES pH 7.4, 150 mM NaCl, 5% glycerol and 7.5 mM glutaraldehyde, and incubated 5 min;
225 then glutaraldehyde was quenched for 5 min by addition of 1M Tris stock to a final concentration
226 of 75 mM. A 5-µl drop of sample was applied to a glow-discharged, carbon-coated grid for 10-15
227 s, blotted, stained with 2% uranyl formate, blotted and air-dried. Images were obtained with a
228 Philips EM420 electron microscope at 120 kV, 82,000× magnification, and a 4.02 Å pixel size.
229 The RELION program [17] was used for particle picking, 2D and 3D class averaging.

230 *Thermostability assays*

231 Thermostability of the S ectodomain samples were measured using DSF and DSC.
232 Samples were purified and buffer exchanged into HBS buffer (10 mM HEPES, 150 mM NaCl,
233 pH 7.4) by SEC on a Superose 6 10/300 column. DSF assay was performed using Tycho NT. 6
234 (NanoTemper Technologies). Spike variants were diluted (0.15 mg/ml) in HBS and run in
235 triplicate. Intrinsic fluorescence was recorded at 330 nm and 350 nm while heating the sample
236 from 35–95 °C at a rate of 30 °C/min. The ratio of fluorescence (350/330 nm) and inflection
237 temperatures (Ti) were calculated by Tycho NT. 6.

238 DSC measurements were performed using the NanoDSC platform (TA instruments; New
239 Castle, DE). Samples that had been incubated at 22 ºC or 37 ºC were purified by SEC at room
240 temperature and the sample incubated at 4 ºC was purified by SEC at 4 ºC (Extended Data Figure
241 2), diluted to 0.2–0.3 mg/mL in HBS, and degassed for 15 min at room temperature prior to
242 analysis. DSC measurements were performed immediately after SEC purification of the

243 samples. DSC cells were conditioned with filtered, degassed HBS prior to sample loading.
244 Protein samples were heated from 10 °C to 100 °C at 1 °C/min under 3 atm pressure using HBS
245 as the reference buffer. The observed denaturation profiles were buffer subtracted, converted to
246 molar heat capacity, baseline-corrected with a 6th-order polynomial, and fit with 2-4 Gaussian
247 transition models, as needed, using the NanoAnalyze software (TA Instruments). The peak
248 transition temperature (T_m) is reported as the temperature at the maximum observed heat
249 capacity of each transition peak.

250 *Isolation of antibodies from COVID-19 convalescent donors*

251 Human SARS-CoV-2 Spike antibodies Ab712199 and Ab511584 were isolated from a COVID-
252 19 convalescent individual. Peripheral blood was collected following informed consent on a
253 Duke University Medical Center approved Institutional Review Board protocol. Briefly, PBMC
254 samples collected after the onset of the symptoms were stained and the memory B cells were
255 sorted with SARS-CoV-2 Spike-2p probes. Antibody IgH and IgK/L genes were recovered from
256 the single-cell sorted cells, cloned into human IgG1 constant region backbone, and purified by
257 Protein A beads as previously described [18].

258 *ELISA assays*

259 Spike samples were pre-incubated at different temperatures then tested for antibody- or ACE-2-
260 binding in ELISA assays as previously described [19,20]. Assays were run in two formats. In the
261 first format antibodies or ACE-2 protein were coated on 384-well plates at 2 µg/ml overnight at
262 4°C, washed, blocked and followed by two-fold serially diluted spike protein starting at 25 µg/ml.
263 Binding was detected with polyclonal anti-SARS-CoV-2 spike rabbit serum (developed in our
264 lab), followed by goat anti-rabbit-HRP (Abcam #ab97080) and TMB substrate (Sera Care Life
265 Sciences #5120-0083). Absorbance was read at 450 nm. In the second format, serially diluted
266 spike protein was bound in individual wells of 384-well plates, which were previously coated with
267 streptavidin (Thermo Fisher Scientific #S-888) at 2 µg/ml and blocked. Proteins were incubated

268 at room temperature for 1 hour, washed, then human mAbs were added at 10 µg/ml. Antibodies
269 were incubated at room temperature for 1 hour, washed and binding detected with goat anti-
270 human-HRP (Jackson ImmunoResearch Laboratories, #109-035-098) and TMB substrate.

271 Commercially obtained constructs of SARS-CoV-2 spike ectodomain (S1+S2 ECD, S2
272 ECD and RBD) (Sino Biological Inc cat# 40589-V08B1 and 40590-V08B respectively and RBD
273 from Genescript cat# Z03483) were coated directly on 384-well plates at 2 µg/ml and incubated
274 overnight at 4 ^{o}C. Plates were washed, blocked and human mAbs three-fold serially diluted from
275 100 µg/ml were added for 1 hour at room temp followed by washing. Binding was detected with
276 Goat anti-human IgG-HRP followed by TMB substrate.
277

278 *Microneutralization assay*

279 Live SARS-CoV-2 Microneutralization (MN) assays were adapted from Berry et al.[21] In short,
280 sera or purified antibodies are diluted two-fold and incubated with 100 TCID50 virus for 1 hour.
281 These dilutions are used as the input material for a TCID50. Each batch of MN includes known
282 neutralizing and non-neutralizing controls. Data are reported as the last concentration at which a
283 test sample protects Vero E6 cells. Recently, a fluorescent infectious clone of SARS-CoV-2 was
284 developed[22].

285 *Plaque Reduction Neutralization Test (PRNT)*

286 Live SARS-CoV-2 Plaque Reduction Neutralization Test (PRNT) was performed in an assay
287 adapted from Berry et al.[21] Briefly, two-fold dilutions of a test sample (serum, plasma, purified
288 Ab) are incubated with 50 PFU SARS-CoV-2 for 1 hour (NR-52281; BEI Resources). The
289 antibody/virus mixture was then used to inoculate Vero E6 cells (ATCC). Cultures were then
290 incubated at 37°C, 5% CO_2 for one hour. At the end of the incubation, 1 mL of a viscous overlay
291 (1:1 2X DMEM and 1.2% methylcellulose) was added to each well. Plates were incubated for 4
292 days. After fixation, staining and washing, plates were dried and plaques counted. Known

293 neutralizing and non-neutralizing antibodies/sera are included in this assay as positive and
294 negative controls, respectively. Plaques from each dilution of each sample are counted and
295 data are reported as the concentration at which 50% of input virus is neutralized.
296
297 *Pseudovirus Neutralization Assay*
298 SARS-CoV-2 neutralization was assessed with Spike-pseudotyped viruses in 293T/ACE2 cells
299 as a function of reductions in luciferase (Luc) reporter activity. 293T/ACE2 cells were kindly
300 provided by Drs. Mike Farzan and Huihui Mu at Scripps. Cells were maintained in DMEM
301 containing 10% FBS and 3 µg/ml puromycin. An expression plasmid encoding codon-optimized
302 full-length Spike of the Wuhan-1 strain (VRC7480), was provided by Drs. Barney Graham and
303 Kizzmekia Corbett at the Vaccine Research Center, National Institutes of Health (USA). The
304 D614G amino acid change was introduced into VRC7480 by site-directed mutagenesis using
305 the QuikChange Lightning Site-Directed Mutagenesis Kit from Agilent Technologies (Catalog #
306 210518). The mutation was confirmed by full-length Spike gene sequencing. Pseudovirions
307 were produced in HEK 293T/17 cells (ATCC cat. no. CRL-11268) by transfection using Fugene
308 6 (Promega Cat#E2692) and a combination of Spike plasmid, lentiviral backbone plasmid
309 (pCMV ΔR8.2) and firefly Luc reporter gene plasmid (pHR' CMV Luc)[23] in a 1:17:17 ratio.
310 Transfections were allowed to proceed for 16-20 hours at 37°C. Medium was removed,
311 monolayers rinsed with growth medium, and 15 ml of fresh growth medium added. Pseudovirus-
312 containing culture medium was collected after an additional 2 days of incubation and was
313 clarified of cells by low-speed centrifugation and 0.45 µm micron filtration and stored in aliquots
314 at -80°C. $TCID_{50}$ assays were performed on thawed aliquots to determine the infectious dose for
315 neutralization assays (RLU 500-1000x background, background usually averages 50-100 RLU).
316
317 For neutralization, a pre-titrated dose of virus was incubated with 8 serial 3-fold or 5-fold
318 dilutions of serum samples or mAbs in duplicate in a total volume of 150 µl for 1 hr at 37°C in

319 96-well flat-bottom poly-L-lysine-coated culture plates (Corning Biocoat). Cells were suspended
320 using TrypLE express enzyme solution (Thermo Fisher Scientific) and immediately added to all
321 wells (10,000 cells in 100 µL of growth medium per well). One set of 8 control wells received
322 cells + virus (virus control) and another set of 8 wells received cells only (background control).
323 After 66-72 hrs of incubation, medium was removed by gentle aspiration and 30 µL of Promega
324 1X lysis buffer was added to all wells. After a 10 minute incubation at room temperature, 100 µL
325 of Bright-Glo luciferase reagent was added to all wells. After 1-2 minutes, 110 µL of the cell
326 lysate was transferred to a black/white plate (Perkin-Elmer). Luminescence was measured
327 using a PerkinElmer Life Sciences, Model Victor2 luminometer. Neutralization titers are the
328 serum dilution (ID50/ID80) or mAb concentration (IC50/IC80) at which relative luminescence
329 units (RLU) were reduced by 50% and 80% compared to virus control wells after subtraction of
330 background RLUs. Maximum percent inhibition (MPI) is the % neutralization at the lowest serum
331 dilution or highest mAb concentration tested. Serum samples were heat-inactivated for 30
332 minutes at 56 ^{o}C prior to assay.

333 *Surface Plasmon Resonance*

334 Antibody binding to SARS-CoV-2 spike constructs was assessed by surface plasmon
335 resonance on a Biacore T-200 (GE-Healthcare) with HBS buffer with 3 mM EDTA and 0.05%
336 surfactant P-20 added. For the data presented in Figure 1H and Supplementary Figure 2, spike
337 samples that were incubated at 4 ºC, 22 ºC and 37 ºC for a week, were held in the sample
338 chamber at 8 ºC, 22 ºC and 37 ºC, respectively, during the SPR run. For the SPR data
339 presented in Extended Data Figures 4 and 7, the sample incubated at 4 ºC for a week was held
340 in the sample chamber at 8 ºC, and the samples incubated at 22 ºC and 37 ºC for a week, were
341 held in the sample chamber at 22 ºC during the run. The flow cell was maintained at 25 ºC, thus
342 all binding assays were performed at 25 ºC. Antibodies captured on a CM5 chip coated with
343 amine-coupled human Anti-Fc (8000RU) were assayed by SARS-CoV-2 spike at 200 nM. The

344 surface was regenerated between injections with 3 M $MgCl_2$ solution for 10 s at 100 µl/min.

345 Sensorgram data were analyzed using the BiaEvaluation software (GE Healthcare).

346

347 *Cryo-EM*

348 Purified SARS-CoV-2 spike preparations were diluted to a concentration of ~1 mg/mL in 2 mM

349 Tris pH 8.0, 200 mM NaCl and 0.02% NaN_3. A 2.5-µL drop of protein was deposited on a CF-

350 1.2/1.3 grid that had been glow discharged for 30 seconds in a PELCO easiGlow™ Glow

351 Discharge Cleaning System. After a 30 s incubation in >95% humidity, excess protein was

352 blotted away for 2.5 seconds before being plunge frozen into liquid ethane using a Leica EM

353 GP2 plunge freezer (Leica Microsystems). Frozen grids were imaged in a Titan Krios (Thermo

354 Fisher) equipped with a K3 detector (Gatan).

355 **Data Availability**

356 The datasets generated the current study are available from the corresponding author on
357 reasonable request.

References

1 Wrapp, D. *et al.* Cryo-EM structure of the 2019-nCoV spike in the prefusion conformation. *Science* **367**, 1260-1263, doi:10.1126/science.abb2507 (2020).

2 Walls, A. C. *et al.* Structure, Function, and Antigenicity of the SARS-CoV-2 Spike Glycoprotein. *Cell* **181**, 281-292 e286, doi:10.1016/j.cell.2020.02.058 (2020).

3 Barnes, C. O. *et al.* Structures of human antibodies bound to SARS-CoV-2 spike reveal common epitopes and recurrent features of antibodies. *bioRxiv*, doi:10.1101/2020.05.28.121533 (2020).

4 Pinto, D. *et al.* Cross-neutralization of SARS-CoV-2 by a human monoclonal SARS-CoV antibody. *Nature*, doi:10.1038/s41586-020-2349-y (2020).

5 Mire, C. E. *et al.* A Cross-Reactive Humanized Monoclonal Antibody Targeting Fusion Glycoprotein Function Protects Ferrets Against Lethal Nipah Virus and Hendra Virus Infection. *J Infect Dis* **221**, S471-S479, doi:10.1093/infdis/jiz515 (2020).

6 Ke, Z., Oton, J.; Qu, K.; Cortese, M.; Zila, V.; McKeane, L.; Nakane, T.; Zivanov, J.; Neufeldt, C.J.; Lu, J.M.; Peukes, J.; Xiong, X.; Krausslich, H.G.; Scheres, S.H.W.; Bartenschlager, R.; Briggs, J.A.G. Structures, conformations and distributions of SARS-CoV-2 spike protein trimers on intact virions. *bioRxiv* (2020).

7 Liu, L. *et al.* Potent Neutralizing Monoclonal Antibodies Directed to Multiple Epitopes on the SARS-CoV-2 Spike. *bioRxiv*, doi:10.1101/2020.06.17.153486 (2020).

8 Zhou, T. *et al.* Structure-Based Design with Tag-Based Purification and In-Process Biotinylation Enable Streamlined Development of SARS-CoV-2 Spike Molecular Probes. *bioRxiv*, doi:10.1101/2020.06.22.166033 (2020).

9 Henderson, R. *et al.* Controlling the SARS-CoV-2 spike glycoprotein conformation. *Nat Struct Mol Biol*, doi:10.1038/s41594-020-0479-4 (2020).

10 Magnusson, A. O. *et al.* nanoDSF as screening tool for enzyme libraries and biotechnology development. *FEBS J* **286**, 184-204, doi:10.1111/febs.14696 (2019).

11 Hsieh, C. L. *et al.* Structure-based design of prefusion-stabilized SARS-CoV-2 spikes. *Science*, doi:10.1126/science.abd0826 (2020).

12 Zhou, T. *et al.* A pH-dependent switch mediates conformational masking of SARS-CoV-2 spike. *bioRxiv*, doi:10.1101/2020.07.04.187989 (2020).

13 Good, N. E. *et al.* Hydrogen ion buffers for biological research. *Biochemistry* **5**, 467-477, doi:10.1021/bi00866a011 (1966).

14 Acharya, P. *et al.* A glycan cluster on the SARS-CoV-2 spike ectodomain is recognized by Fab-dimerized glycan-reactive antibodies. *bioRxiv*, doi:10.1101/2020.06.30.178897 (2020).

15 Xiong, X. *et al.* A thermostable, closed SARS-CoV-2 spike protein trimer. *Nat Struct Mol Biol*, doi:10.1038/s41594-020-0478-5 (2020).

16 Henderson, R. *et al.* Glycans on the SARS-CoV-2 Spike Control the Receptor Binding Domain Conformation. *bioRxiv*, doi:10.1101/2020.06.26.173765 (2020).

17 Scheres, S. H. W. in *Methods in Enzymology* Vol. 579 (ed R. A. Crowther) 125-157 (Academic Press, 2016).

18 Liao, H. X. *et al.* Co-evolution of a broadly neutralizing HIV-1 antibody and founder virus. *Nature* **496**, 469-476, doi:10.1038/nature12053 (2013).

19 Alam, S. M. *et al.* Mimicry of an HIV broadly neutralizing antibody epitope with a synthetic glycopeptide. *Science translational medicine* **9**, doi:10.1126/scitranslmed.aai7521 (2017).

20 Bonsignori, M. *et al.* Staged induction of HIV-1 glycan-dependent broadly neutralizing antibodies. *Science translational medicine* **9**, doi:10.1126/scitranslmed.aai7514 (2017).

406 21 Berry, J. D. *et al.* Development and characterisation of neutralising monoclonal antibody
407 to the SARS-coronavirus. *J Virol Methods* **120**, 87-96,
408 doi:10.1016/j.jviromet.2004.04.009 (2004).
409 22 Xie, X. *et al.* An Infectious cDNA Clone of SARS-CoV-2. *Cell Host Microbe* **27**, 841-848
410 e843, doi:10.1016/j.chom.2020.04.004 (2020).
411 23 Naldini, L. *et al.* In vivo gene delivery and stable transduction of nondividing cells by a
412 lentiviral vector. *Science* **272**, 263-267, doi:10.1126/science.272.5259.263 (1996).

413

414

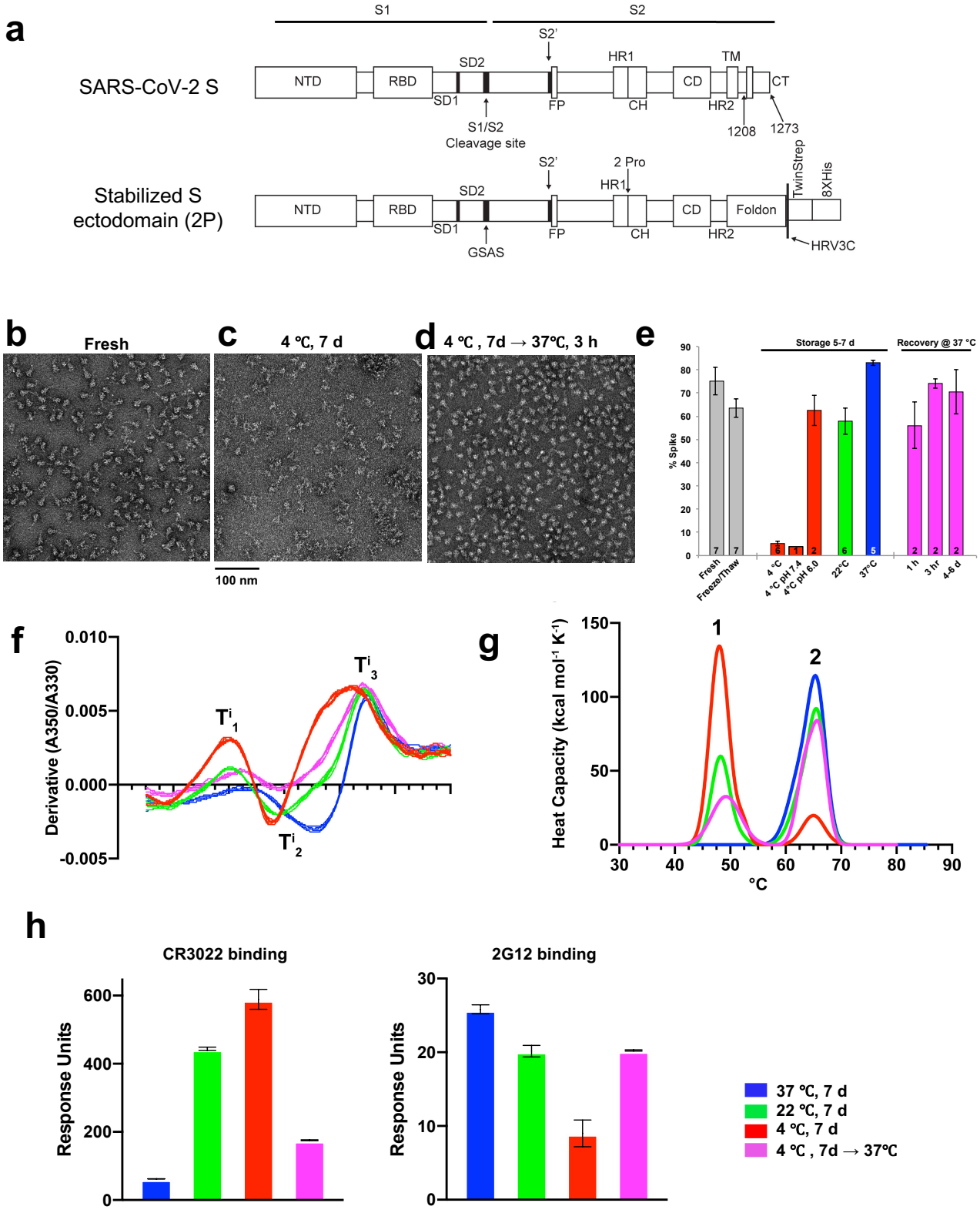
a
S1
S2
S2'
SARS-CoV-2 S
NTD
RBD
SD2
SD1
S1/S2
Cleavage site
FP
HR1
CH
CD
TM
HR2
CT
1208
1273
Stabilized S
ectodomain (2P)
2 Pro
GSAS
Foldon
TwinStrep
8XHis
HRV3C
b
Fresh
c
4 ℃, 7 d
d
4 ℃ , 7d → 37℃, 3 h
100 nm
e
Storage 5-7 d
Recovery @ 37 °C
% Spike
Fresh
Freeze/Thaw
4 °C
4 °C pH 7.4
4°C pH 6.0
22°C
37°C
1 h
3 h
4-6 d
f
Derivative (A350/A330)
Ti1
Ti2
Ti3
g
Heat Capacity (kcal mol-1 K-1)
°C
h
CR3022 binding
2G12 binding
Response Units
37 ℃, 7 d
22 ℃, 7 d
4 ℃, 7 d
4 ℃ , 7d → 37℃

Figure 1. Temperature-dependence of the SARS-CoV-2 S ectodomain. (a) Schematic of the SARS-CoV-2 spike (top) and a furin cleavage-deficient, soluble, stabilized ectodomain construct (bottom). **(b-d)** Representative NSEM micrograph from **(b)** a freshly prepared sample of the S ectodomain, **(c)** the same sample after storing the protein for one week at 4 °C, **(d)** the same sample after storing the protein for one week at 4 °C followed by a 3-hour incubation at 37 °C. **(e)** Bar graph summarizing NSEM results on S ectodomain samples stored under different conditions. From left to right, bars show spike percentage in a fresh sample of spike; after the spike undergoes a single freeze-thaw cycle; after it has been incubated for 5-7 days at 4 °C (red), 22 °C (green) or 37 °C (blue); and spike samples that were stored for 1 week at 4 °C, then incubated at 37 °C for 1 hour, 3 hours, or 4-6 days. Solid bars indicate averages, with number of samples indicated at the bottom of each column. The error bars indicate standard error of the mean, except when N=2, where the error bars indicate range. **(f)** DSF profiles obtained by following changes in intrinsic fluorescence upon applying a thermal ramp to the sample and expressed as the first derivative of the ratio between fluorescence at 350 nm and 330 nm. Maxima and minima indicate inflection temperatures, T^i. For each data point, 5 overlaid curves are shown indicating technical replicates. **(g)** DSC profiles, shown as representative of two technical repeats. **(h)** Antibody CR3022 IgG (left) and 2G12 IgG (right) binding to spike stored at different temperatures measured by SPR. Data for spike samples measured after a 1-week incubation at 37, 22, and 4 °C, are shown in blue, green, and red respectively; sample stored 1 week at 4 °C and then incubated for 6 hours at 37 °C shown in magenta. During the SPR run the sample chamber was maintained at temperatures of 37 °C, 22 °C and 8 °C, for the 37 °C, 22 °C and 4 °C incubated samples, respectively. The binding experiments were carried out at 25 °C. Error bars are derived from 3 technical repeats. The data shown are representative of at least 5 independent experiments. 2 independent repeats using separate protein lots are shown in Supplementary Figure 2.

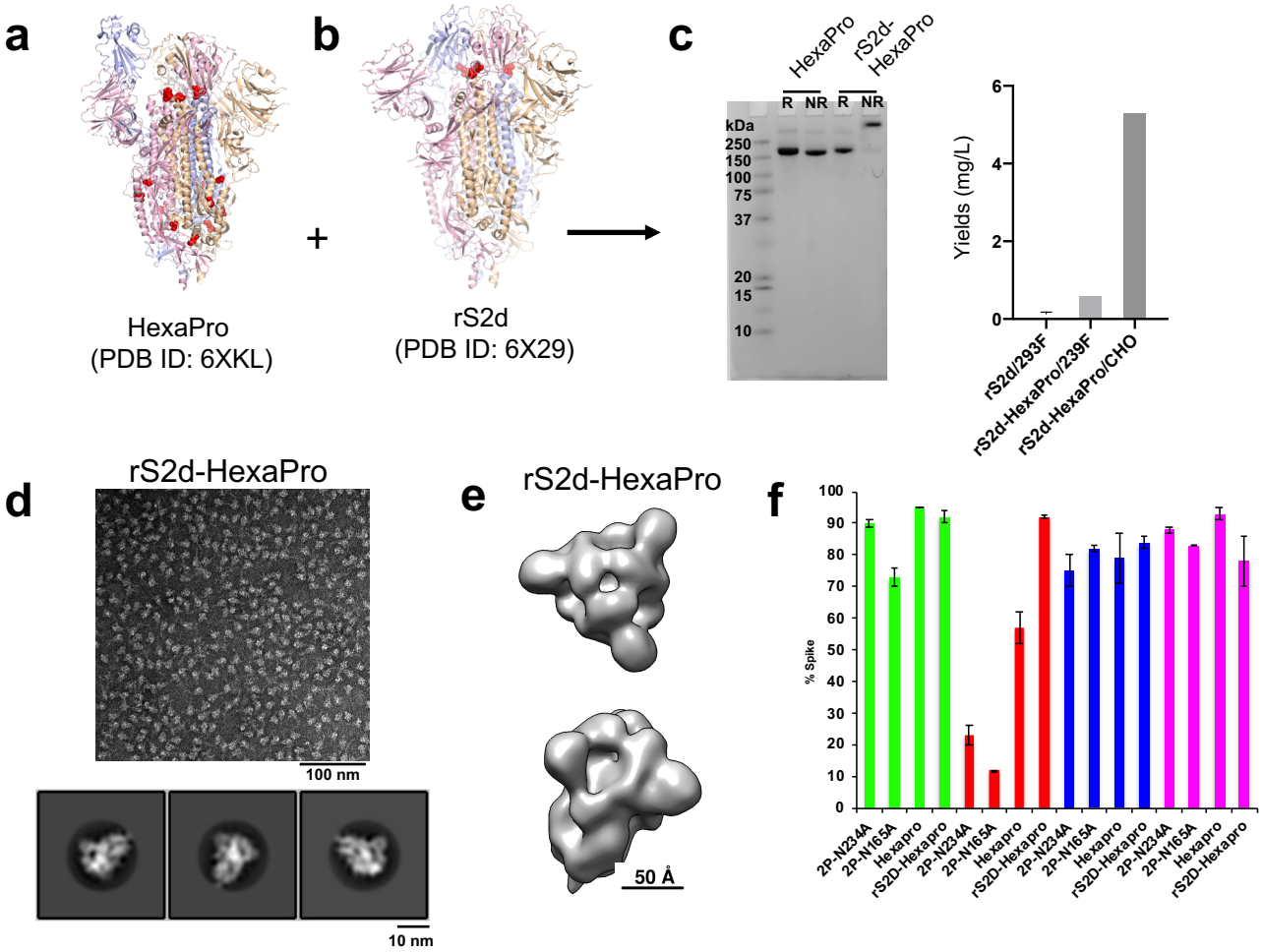
a
HexaPro
(PDB ID: 6XKL)
+
b
rS2d
(PDB ID: 6X29)
c
HexaPro
rS2d-HexaPro
R NR R NR
kDa
250
150
100
75
37
20
15
10
Yields (mg/L)
rS2d/293F
rS2d-HexaPro/239F
rS2d-HexaPro/CHO
d
rS2d-HexaPro
100 nm
10 nm
e
rS2d-HexaPro
50 Å
f
% Spike
2P-N234A
2P-N165A
Hexapro
rS2D-Hexapro

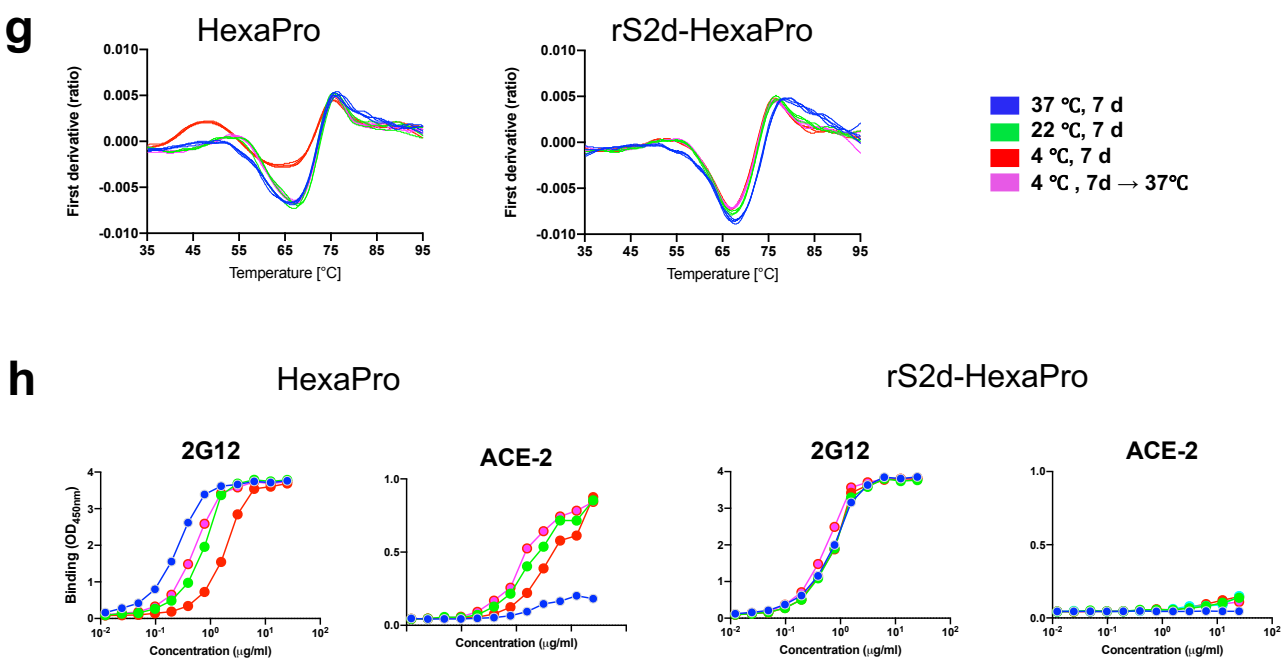
g
HexaPro
rS2d-HexaPro
First derivative (ratio)
Temperature [°C]
37 ℃, 7 d
22 ℃, 7 d
4 ℃, 7 d
4 ℃ , 7d → 37℃
h
HexaPro
rS2d-HexaPro
2G12
ACE-2
Binding (OD450nm)
Concentration (μg/ml)

Figure 2. Engineered SARS-CoV-2 spike variant, rS2d-HexaPro, is resistant to temperature-dependent structural changes. (a-b) Structures of **(a)** HexaPro showing a 1-RBD-up conformation (PDB ID: 6X29) and **(b)** rS2d (PDB ID: 6XKL) showing a all-RBD-down conformation. **(c)** *(left)* SDS-PAGE. Lane 1: Molecular weight marker, Lanes 2 and 3: HexaPro, Lane 4 and 5: rS2d-HexaPro. R= Reducing, and NR = Non-reducing conditions. *(right)* Bar graph summarizing protein yields in mg/L of culture for, from left to right, rS2d produced in 293F cells, rS2d-HexaPro produced in Freestyle 293F cells, and rS2d-HexaPro expressed in CHO cells. **(d)** *(top)* Representative NSEM micrograph from a preparation of rS2d-Hexapro and *(bottom)* 2D class averages. **(e)** 3D reconstruction of rS2d-Hexapro obtained from NSEM data. **(f)** Bar graph summarizing results from NSEM on spike variants stored at different temperatures. Error bars shown are derived from at least two independent experiments with dfferent protein lots, and represent standard error of mean where N ≥ 3 and range where N=2. **(g)** DSF profiles for Hexapro (left) and rS2d-Hexapro (right). **(h)** Binding of 2G12 and ACE-2 to Hexapro (left) and rS2d-Hexapro (right) measured by ELISA. Serially diluted spike protein was bound in individual wells of 384-well plates, which were previously coated with streptavidin. Proteins were incubated and washed, then 2G12 at 10 µg/ml or ACE-2 with a mouse Fc tag at 2 µg/ml were added. Antibodies were incubated, washed and binding detected with goat anti-human-HRP.

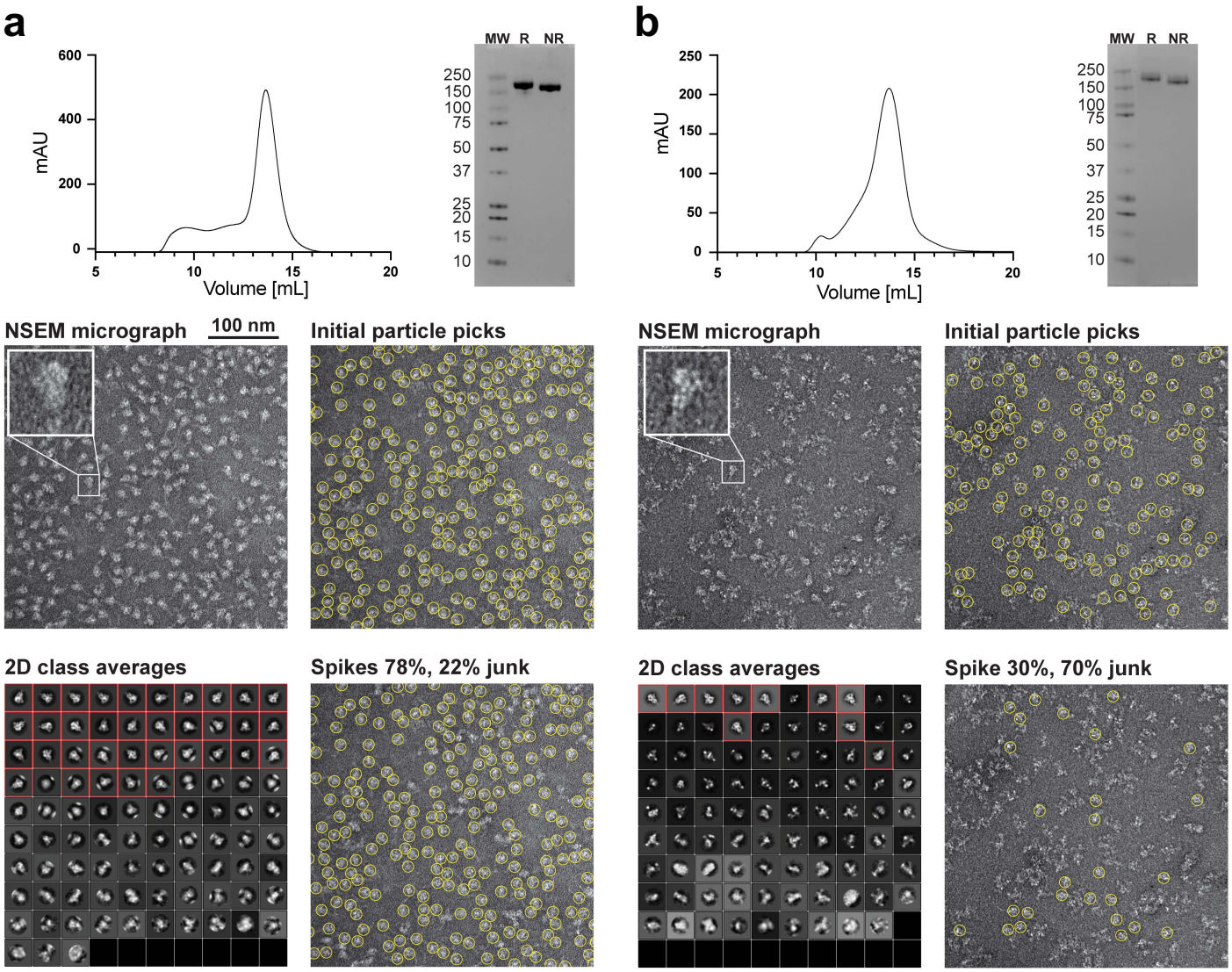

Extended Data Figure 1. Purification and quality control of the SARS-CoV-2 S protein ectodomain. (a and b) Two representative spike preparations that together highlight the role of NSEM in discriminating between good **(a)** and bad **(b)** spike preparations that otherwise appear to be of similar quality by SEC (top, left) and SDS-PAGE (top, right). Representative micrographs from each prep are shown, middle left. Protein appears as white blobs on gray background. Insets show a single kite-shaped spike particle enlarged. At the middle right, automatic particle picking is shown as yellow circles superimposed on the micrograph. Sets of ~20,000 initial particles picks are subjected to automated 2D classification to group together and average particles with similar features into discrete classes, bottom left. In the 2D class averages for each sample, the classes that contain the SARS-Cov-2 S ectodomain (shown within red boxes) can be clearly distinguished from classes that contain junk. The final spike picks come from the particles contained within the indicated classes and their total number provide an estimate of the ratio between the SARS-CoV-2 S ectodomain and junk seen in the NSEM sample.

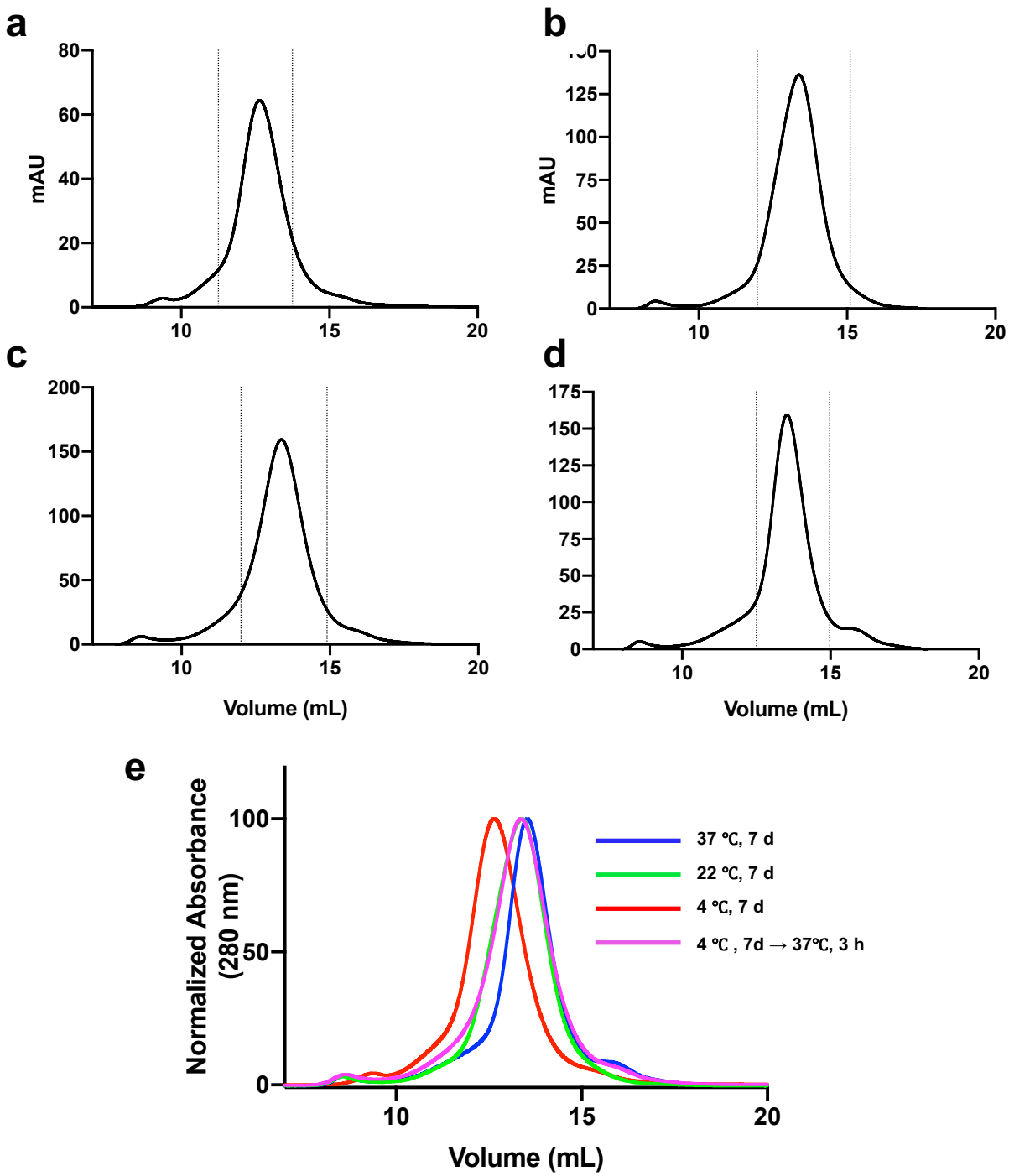

Extended Data Figure 2. Size Exclusion Chromatography of SARS-CoV-2 S ectodomain incubated at different temperatures. SEC profiles run on a Superose 6 increase 10/300 column for SARS-CoV-2 S ectodomain samples that were incubated at **(a)** 4 °C for one week, **(b)** 22 °C for one week. **(c)** 37 °C for one week, and **(d)** 4 °C for one week and moved to 37 °C for 3 hours prior to the experiment. **(e)** Overlay of SEC plots normalized to allow better visualization of peak shifts.

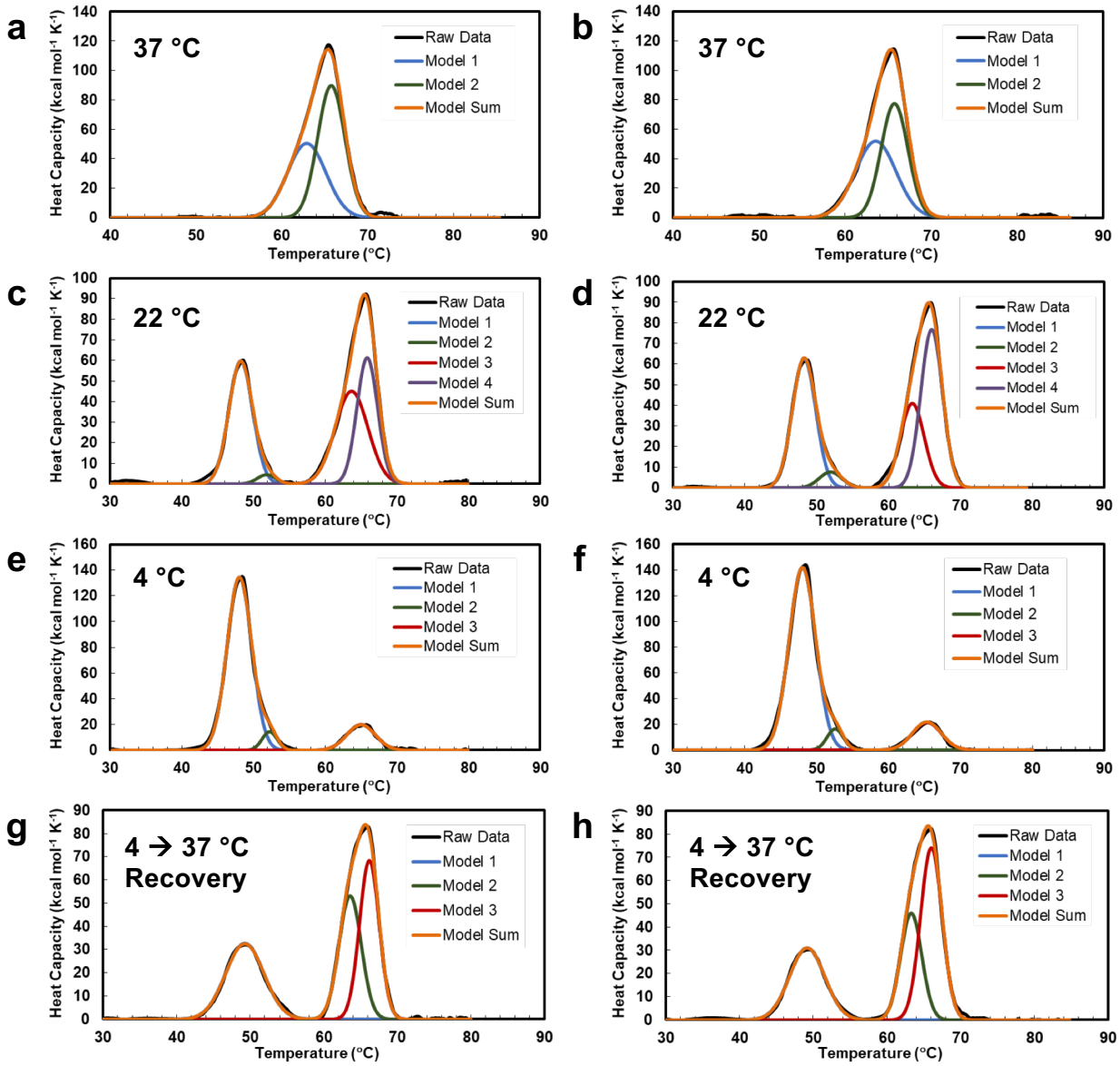

i

	Transition Peak 1		Transition Peak 2		DSC Model Fits			
	T_{onset} (°C)	T_m (°C)	T_{onset} (°C)	T_m (°C)	$T_{m,1}$ (°C)	$T_{m,2}$ (°C)	$T_{m,3}$ (°C)	$T_{m,4}$ (°C)
37 °C	N/A	**N/A**	57.5 ± 0.4	**65.5 ± 0.2**	63.2 ± 0.7	65.74 ± 0.02	N/A	N/A
22 °C	43.64 ± 0.02	**48.2 ± 0.1**	59 ± 1	**65.8 ± 0.1**	48.2 ± 0.1	51.87 ± 0.03	63.5 ± 0.5	65.9 ± 0.1
4 °C	43.0 ± 0.4	**48.41 ± 0.01**	61.1 ± 0.2	**65.1 ± 0.3**	48.02 ± 0.03	52.4 ± 0.3	65.1 ± 0.3	N/A
4 → 37 °C Recovery	42.5 ± 0.5	**49.2 ± 0.1**	59.59 ± 0.04	**65.95 ± 0.02**	49.2 ± 0.1	63.4 ± 0.3	66.1 ± 0.2	N/A

Extended Data Figure 3. Thermostability of the SARS-CoV-2 spike ectodomain stored at different temperatures. Representative thermal denaturation profiles of the SARS-CoV-2 spike ectodomain after 1 week incubations at (**a,b**) 37 °C , (**c,d**) 22 °C, (**e,f**) 4 °C, and (**g,h**) 4 °C followed by 37 °C for 3 hours. Profiles and transition parameters (**I**) were obtained by DSC and analyzed as described in Methods. Raw data (black) was best fit with two or more Gaussian transition models ($T_{m,1\text{-}4}$) (blue, green, red, purple). The peak observed at ~65 °C was best fit with two Gaussian transition models suggesting a complex unfolding mechanism. Data shown are the mean and range from two experimental replicates.

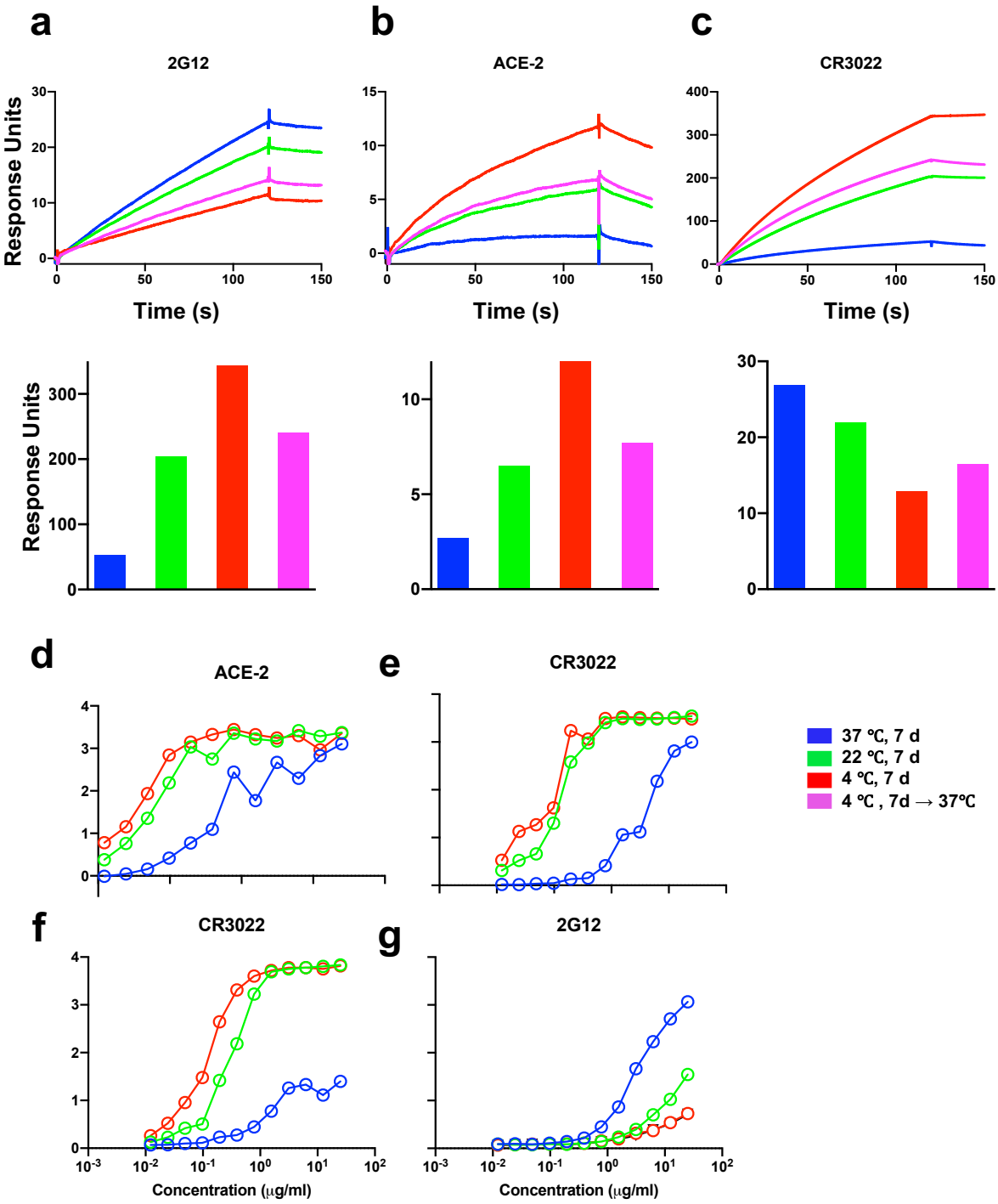

Extended Data Figure 4. Changes in antigenicity of SARS-CoV-2 S ectodomain incubated at different temperatures. (a-c) SPR profiles showing binding of **(a)** ACE-2, **(b)** RBD-directed antibody, CR3022, and **(c)** S2 glycan-directed antibody 2G12 to spike samples incubated for 1 week at either 37 °C (blue), 22 °C (green) or 4 °C (red). Binding to spike sample first incubated at 4 °C for 1 week, then moved to 37 °C for 3 hours prior to the experiment is shown in magenta. **(d-g)** ELISA binding profiles showing binding of **(d)** ACE-2, **(e)** RBD-directed antibody, CR3022, in a format where antibody was coated on the plate (see methods) and **(f)** CR3022 and **(g)** 2G12**,** in a format where spike was captured on a strep-coated plate (see methods).

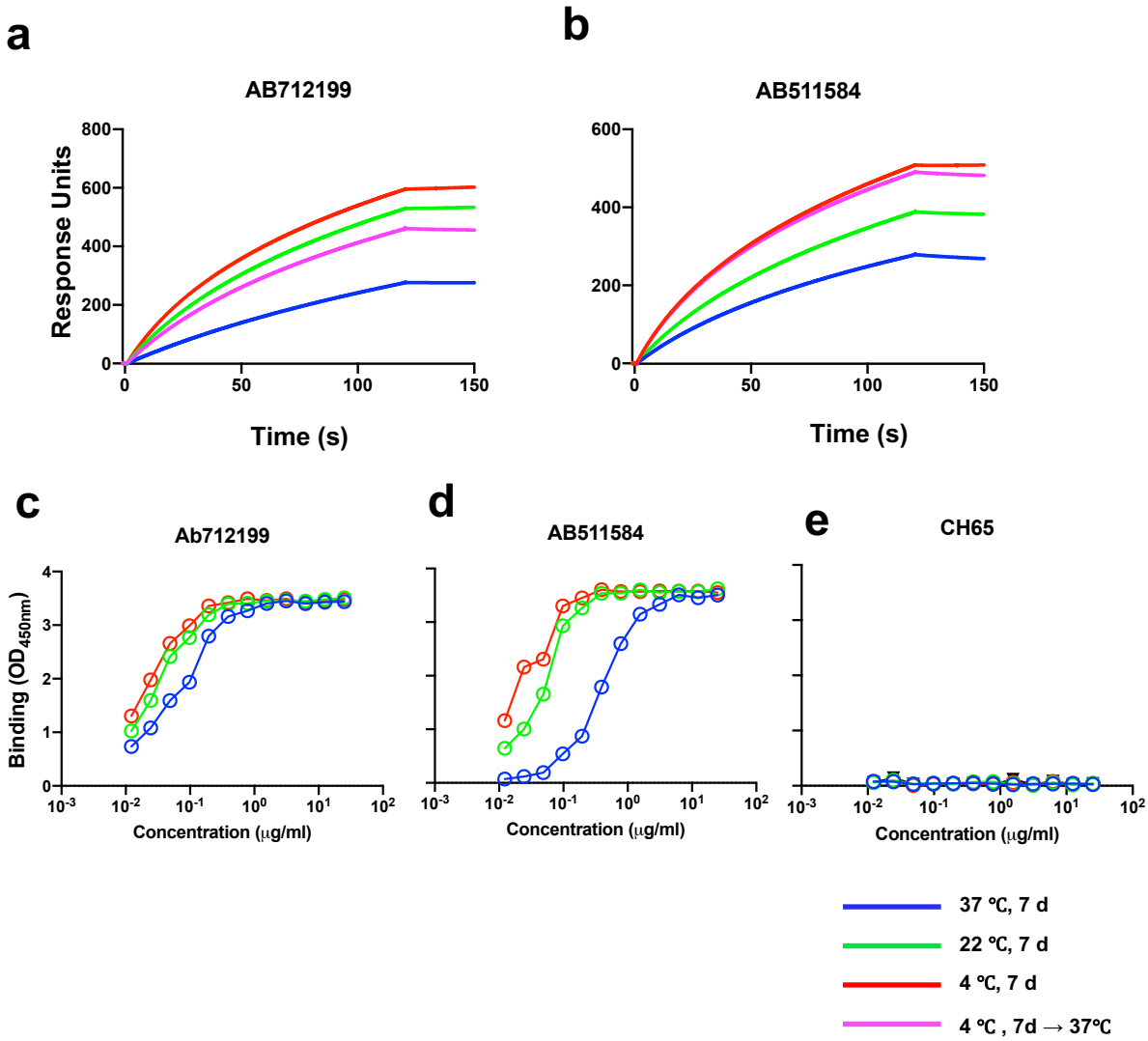

Extended Data Figure 5. Antigenic response of SARS-CoV-2 S ectodomain incubated at different temperatures to antibodies elicited from convalescent patient sera. (**a-b**) SPR binding profiles showing binding of **(a)** RBD-directed antibody, AB712199, **(b)** S2-directed antibody, AB511584 to spike samples incubated for 1 week at either 37 °C (blue), 22 °C (green) or 4 °C (red). Binding to spike sample first incubated at 4 °C for 1 week, then moved to 37 °C for 3 hours prior to the experiment is shown in magenta. **(c-e)** ELISA binding profiles showing binding of **(c)** RBD-directed antibody, AB712199, **(d)** S2-directed antibody, AB511584, or **(e)** influenza HA-directed antibody CH65 (control) to spike samples incubated for 1 week at either 37 °C (blue), 22 °C (green) or 4 °C (red).

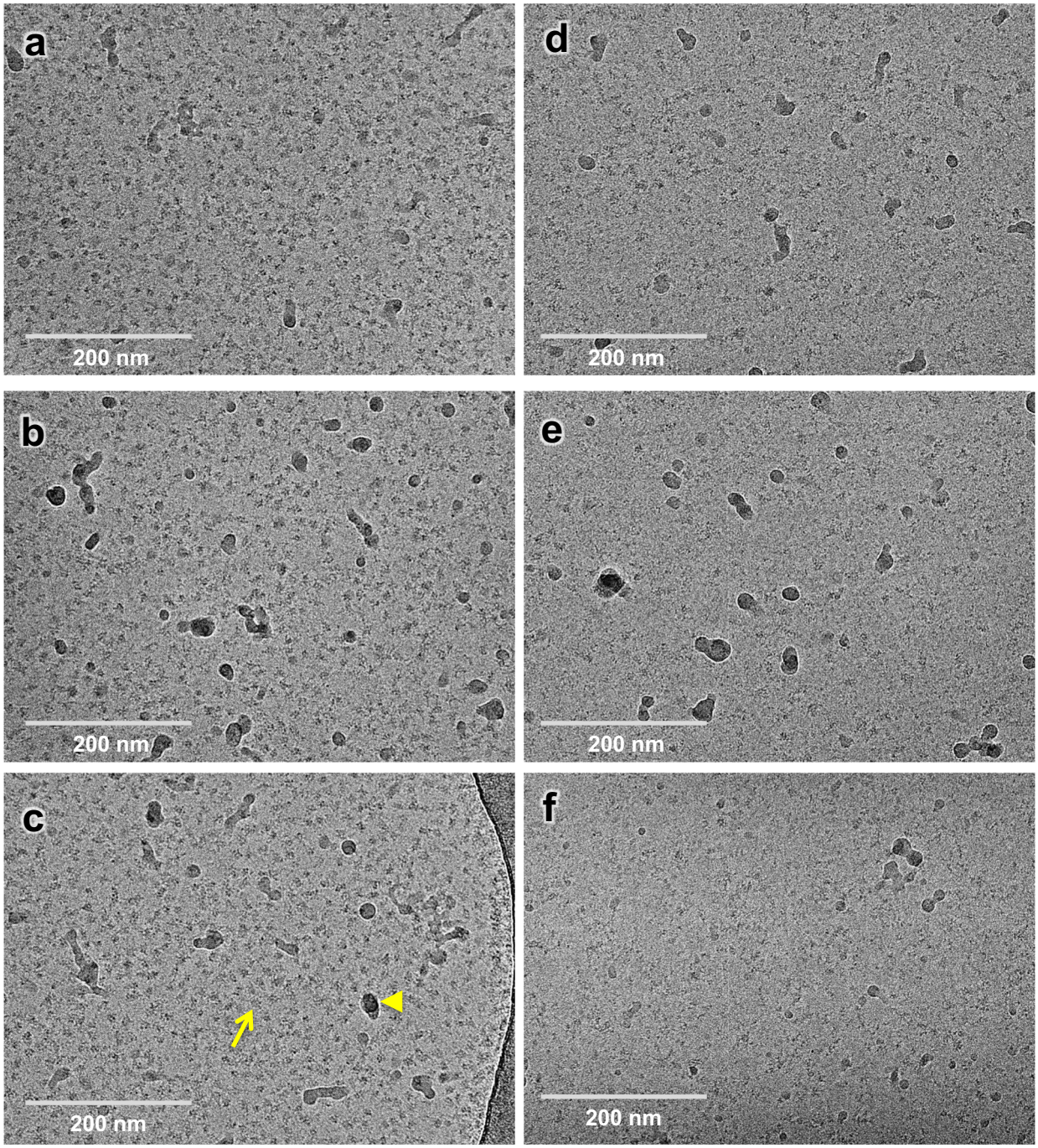

Extended Data Figure 6. Effect of SARS-CoV-2 ectodomain spike sample storage on cryo-EM specimen preparation. (**a-c**) Representative cryo-EM micrographs of a SARS-CoV-2 S ectodomain sample that was flash frozen immediately after purification and stored in -80 °C, then thawed rapidly and incubated for ~ 5 min at 37 °C immediately prior to grid preparation. Cryo-EM images are low contrast, and the desired spike particles appear as medium gray spots (*e.g.* arrow) on a light gray background. Dark gray or black spots are slight ice contamination (*e.g* arrowhead). These panels on the left show an excellent distribution of discrete spike particles. **(d-f)** Representative cryo-EM micrographs of SARS-CoV-2 S ectodomain samples that were stored for ~1 week at 4 °C prior to grid preparation. Compared to the panels of the left, these panels on the right show a sparse field-of-view with very few intact spike particles visible. A similar spike concentration (~1 mg/ml) was used to freeze all the samples. Micrographs were collected on a Titan Krios microscope with a Gatan K3 camera.

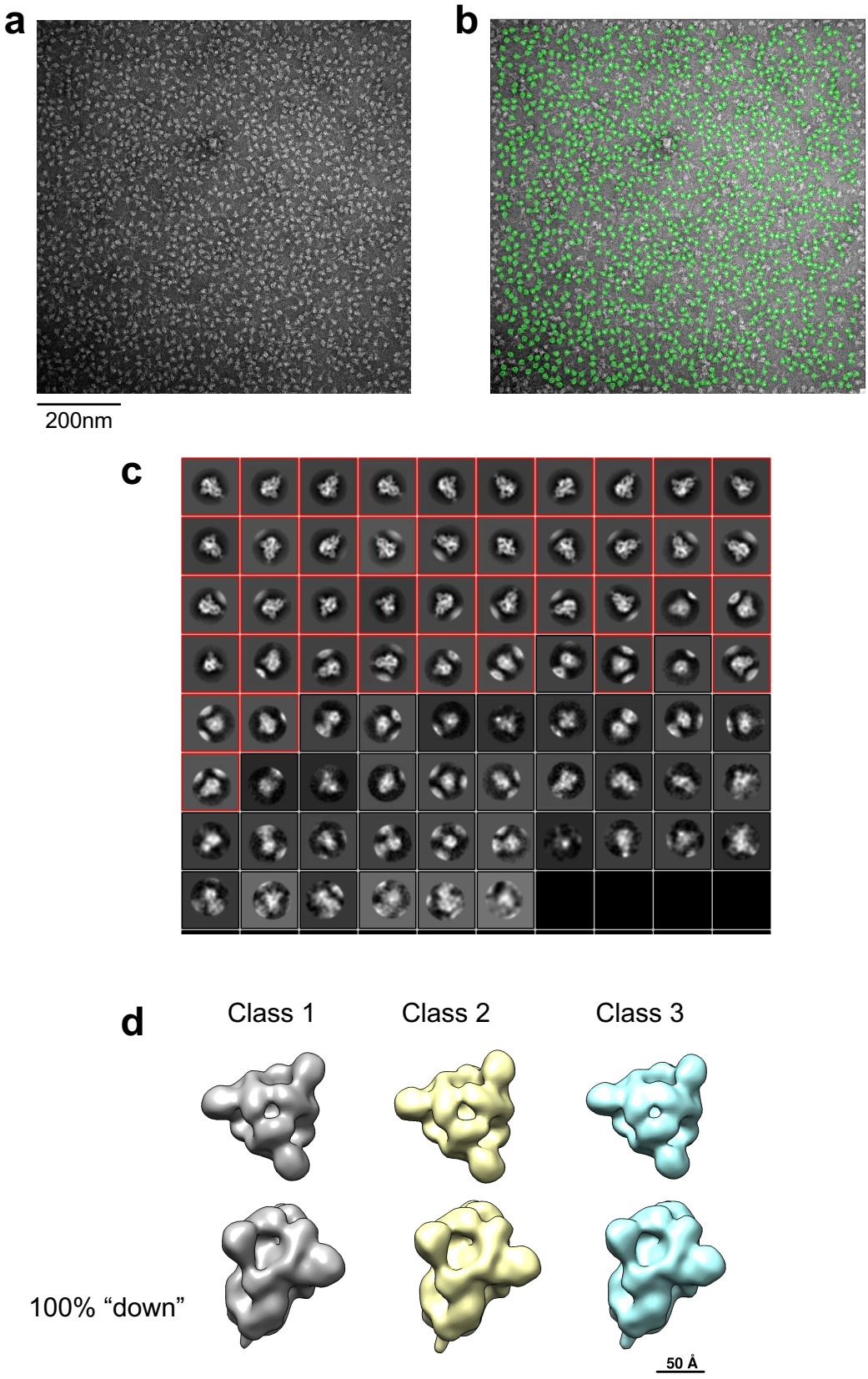
a
b
200nm
c
d
Class 1
Class 2
Class 3
100% “down”
50 Å

Extended Data Figure 7. NSEM workflow for rS2d-HexaPro. (a) Representative NSEM micrograph **(b)** Representative NSEM micrograph showing particle picks in green **(c)** 2D class averages; the particles in the classes marked with a red box were taken forward to the next steps on the analysis **(d)** 3D classes showing top views in the top row and side views in the bottom row. 30,000 particles were used for 3D classification. These were separated into 3 3D classes that were reconstructed using C1 symmetry. Only all-RBD-down classes were observed. Also see Supplementary Movie S1 that shows the residual movement in the RBDs despite being locked down by a RBD-to-S2 disulfide.

Supplementary Table 1. Thermostability of the SARS-CoV-2 spike ectodomain stored at different temperatures measured by DSF. Inflection temperatures from DSF plots shown in Figure 1F, expressed as averages ± standard deviation, N=5.

Storage Temperature	T^i_1	T^i_2	T^i_3
37 °C	53.7 ± 1.1	65 ± 0.2	74.8 ± 0.2
22 °C	49.9 ± 0.2	58.6 ± 0.3	74.2 ± 0.2
4 °C	49.9 ± 0.4	57.5 ± 0.3	71.9 ± 0.2
4->37 °C Recovery	52.2 ± 0.5	58.8 ± 0.5	74.1 ± 0.3

Supplementary Table 2. Thermostability of the SARS-CoV-2 spike ectodomain stored at different temperatures measured by DSC. Table of melting temperatures, T_m, with values expressed as mean ± range, N=2.

Storage Temp.	Transition Peak 1 T_m (°C)	Transition Peak 2 T_m (°C)
37 °C	N/A	65.5 ± 0.2
22 °C	48.2 ± 0.1	65.8 ± 0.1
4 °C	48.41 ± 0.01	65.1 ± 0.3
4 → 37 °C Recovery	49.2 ± 0.1	65.95 ± 0.02

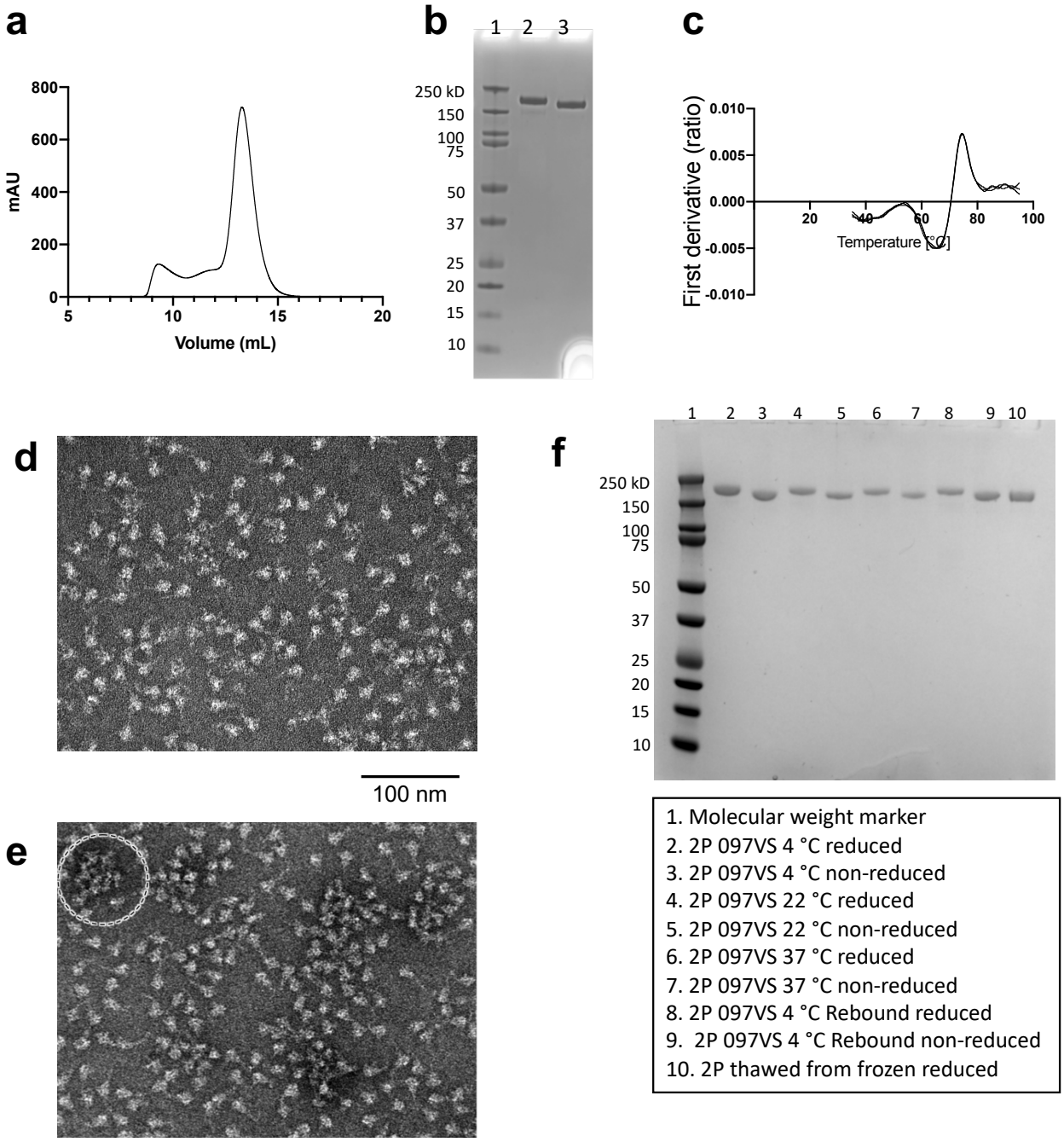

Supplementary Figure 1. SDS-PAGE and NSEM analysis of spike proteins incubated at different temperatures. (a) SEC profile, **(b)** SDS-PAGE analysis (lane 1= molecular weight marker, lane 2= reducing conditions, lane 3= non-reducing conditions) and **(c)** DSF profile of a freshly purified sample of the 2P spike. **(d)** NSEM micrograph of 2P spike after storage at 22 °C for one week. **(e)** NSEM micrograph of 2P spike after storage at 4 °C for one week followed by recovery at 37 °C for 6 days. The circle indicates spike aggregation visible in the micrograph. **(f)** SDS-PAGE analysis of the 2P spike incubated at different temperatures. The legend under the gel lists the sample loaded in each lane. The sample description follows this order- construct name (e.g. 2P), lot # (e.g. 097VS), temperature at which sample was incubated for 1 week (e.g. 4 °C). Samples that were incubated first for 1 week at 4 °C, then moved to 37 °C are labeled as “Rebound”. Reduced and non-reduced sampled are noted. 3 µg sample was loaded in each well.

a

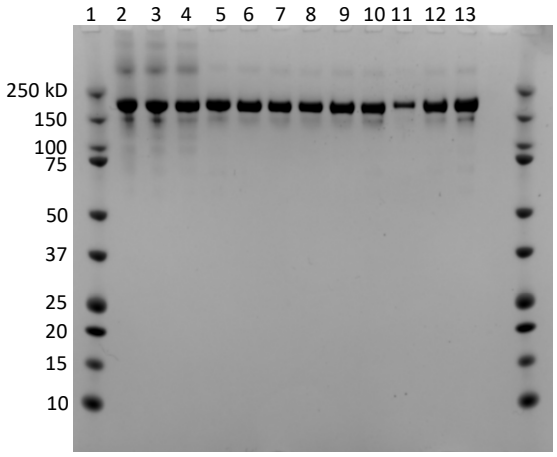

Reduced

1. Molecular weight marker
2. 2P-N165A 095VS 37 °C
3. 2P-N234A 096VS 37 °C Repeat 1
4. 2P-N234A 096VS 37 °C Repeat 2
5. 2P-N165A 095VS 4 °C
6. 2P-N234A 096VS 4 °C Repeat 1
7. 2P-N234A 096VS 4 °C Repeat 2
8. 2P-N165A 095VS 22 °C
9. 2P-N234A 096VS 22 °C Repeat 1
10. 2P-N234A 096VS 22 °C Repeat 2
11. 2P-N165A 095VS 4 °C Rebound
12. 2P-N234A 096VS 4 °C Rebound Repeat 1
13. 2P-N234A 096VS 4 °C Rebound Repeat 2

b

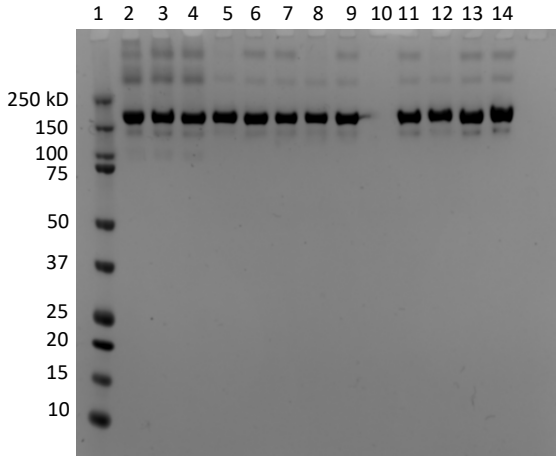

Non-Reduced

1. Molecular weight marker
2. 2P-N165A 095VS 37 °C
3. 2P-N234A 096VS 37 °C Repeat 1
4. 2P-N234A 096VS 37 °C Repeat 2
5. 2P-N165A 095VS 22 °C
6. 2P-N234A 096VS 4 °C Repeat 1
7. 2P-N234A 096VS 4 °C Repeat 2
8. 2P-N165A 095VS 22 °C
9. 2P-N234A 096VS 22 °C Repeat 1
10. Intentionally left blank
11. 2P-N234A 096VS 22 °C Repeat 2
12. 2P-N165A 095VS 4 °C Rebound
13. 2P-N234A 096VS 4 °C Rebound Repeat 1
14. 2P-N234A 096VS 4 °C Rebound Repeat 2

Supplementary Figure 1 (contd). SDS-PAGE analysis of spike proteins incubated at different temperatures. (a) SDS-PAGE under reducing conditions and **(b)** SDS-PAGE under non-reducing conditions. The legend below each gel lists the sample loaded in each lane. The sample description follows this order- construct name (e.g. 2P-N165A), lot # (e.g. 095VS), temperature at which sample was incubated for 1 week (e.g. 4 °C). Samples that were incubated first for 1 week at 4 °C, then moved to 37 °C hours are labeled as “Rebound”. 3 µg sample was loaded in each well.

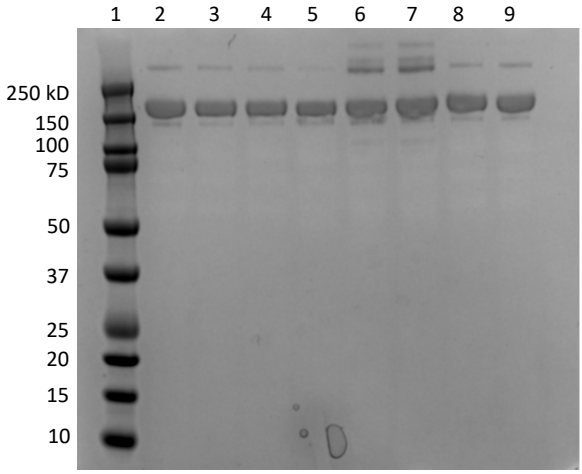

1. Molecular weight marker
2. Hexapro 111KJ 4 °C Repeat 1
3. Hexapro 111KJ 4 °C Repeat 2
4. Hexapro 111KJ 22 °C Repeat 1
5. Hexapro 111KJ 22 °C Repeat 2
6. Hexapro 111KJ 37 °C Repeat 1
7. Hexapro 111KJ 37 °C Repeat 2
8. Hexapro 111KJ 4 °C Rebound Repeat 1
9. Hexapro 111KJ 4 °C Rebound Repeat 2

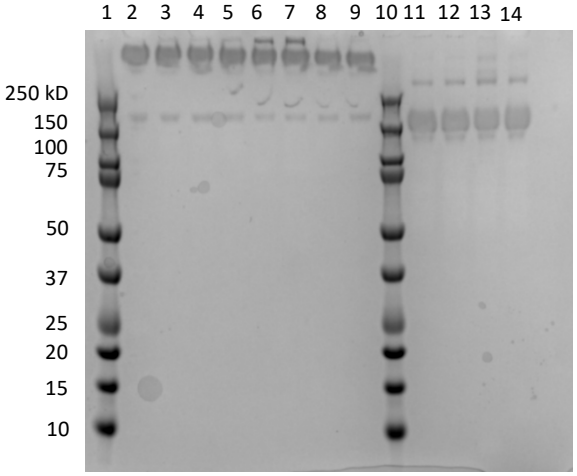

1. Molecular weight marker
2. rS2d-Hexapro 126KJ 4 °C Repeat 1
3. rS2d-Hexapro 126KJ 4 °C Repeat 2
4. rS2d-Hexapro 126KJ 22 °C Repeat 1
5. rS2d-Hexapro 126KJ 22 °C Repeat 2
6. rS2d-Hexapro 126KJ 37 °C Repeat 1
7. rS2d-Hexapro 126KJ 37 °C Repeat 1
8. rS2d-Hexapro 126KJ 4 °C Rebound Repeat 1
9. rS2d-Hexapro 126KJ 4 °C Rebound Repeat 2
10. Molecular weight marker
11. 2P 025MFK 4 °C
12. 2P 025MFK 22 °C
13. 2P 025MFK 37 °C
14. 2P 025MFK 4 °C Rebound

Supplementary Figure 1 (contd). SDS-PAGE analysis of spike proteins incubated at different temperatures. SDS-PAGE under non-reducing conditions. The legend below each gel lists the sample loaded in each lane. The sample description follows this order- construct name (e.g. Hexapro), lot # (e.g. 111KJ), temperature at which sample was incubated for 1 week (e.g. 4 °C). Samples that were incubated first for 1 week at 4 °C, then moved to 37 °C are labeled as "Rebound". 10 µg sample was loaded in each well.

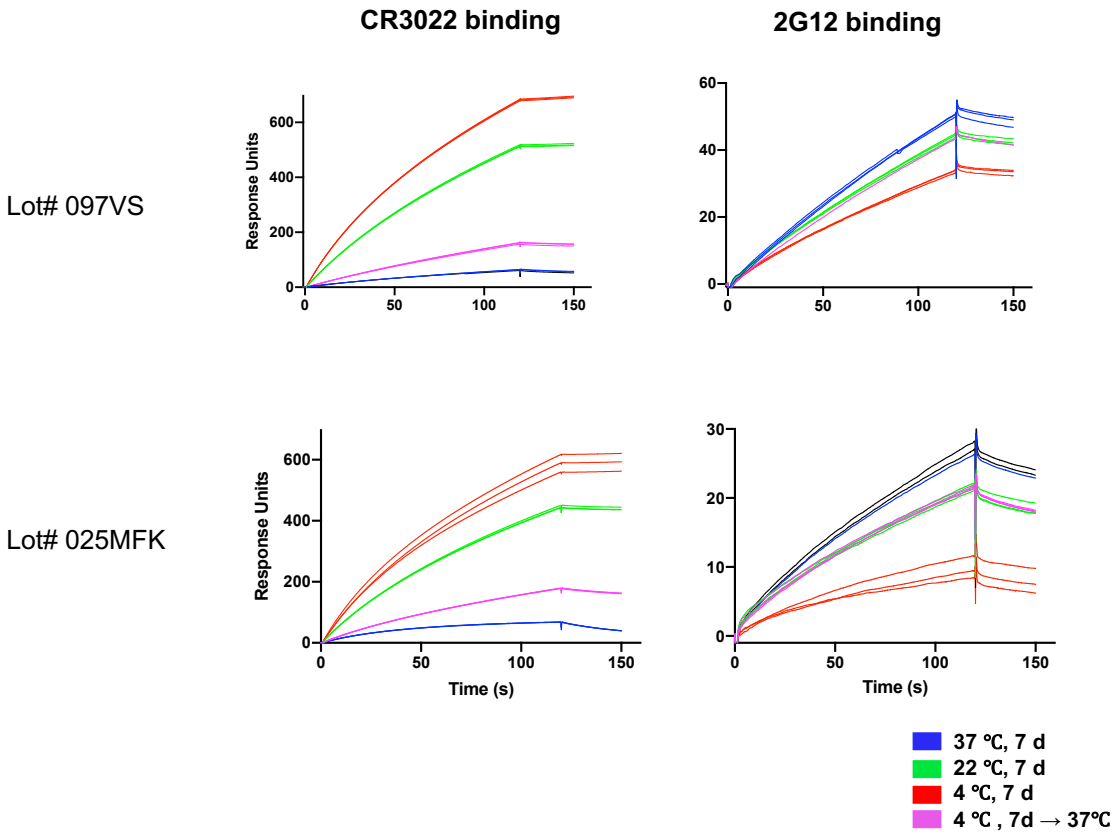

Supplementary Figure 2. Effect of storage temperature on 2P spike antigenicity measured with two different protein lots. Antibody CR3022 IgG (left) and 2G12 IgG (right) binding to spike stored at different temperatures measured by SPR. Data for spike samples measured after a 1-week incubation at 37, 22, and 4 °C, are shown in blue, green, and red respectively; sample stored 1 week at 4 °C and then incubated for 6 hours at 37 °C shown in magenta. During the SPR run the sample chamber was maintained at temperatures of 37 °C, 22 °C and 8 °C, for the 37 °C, 22 °C and 4 °C incubated samples, respectively. The binding experiments were carried out at 25 °C.

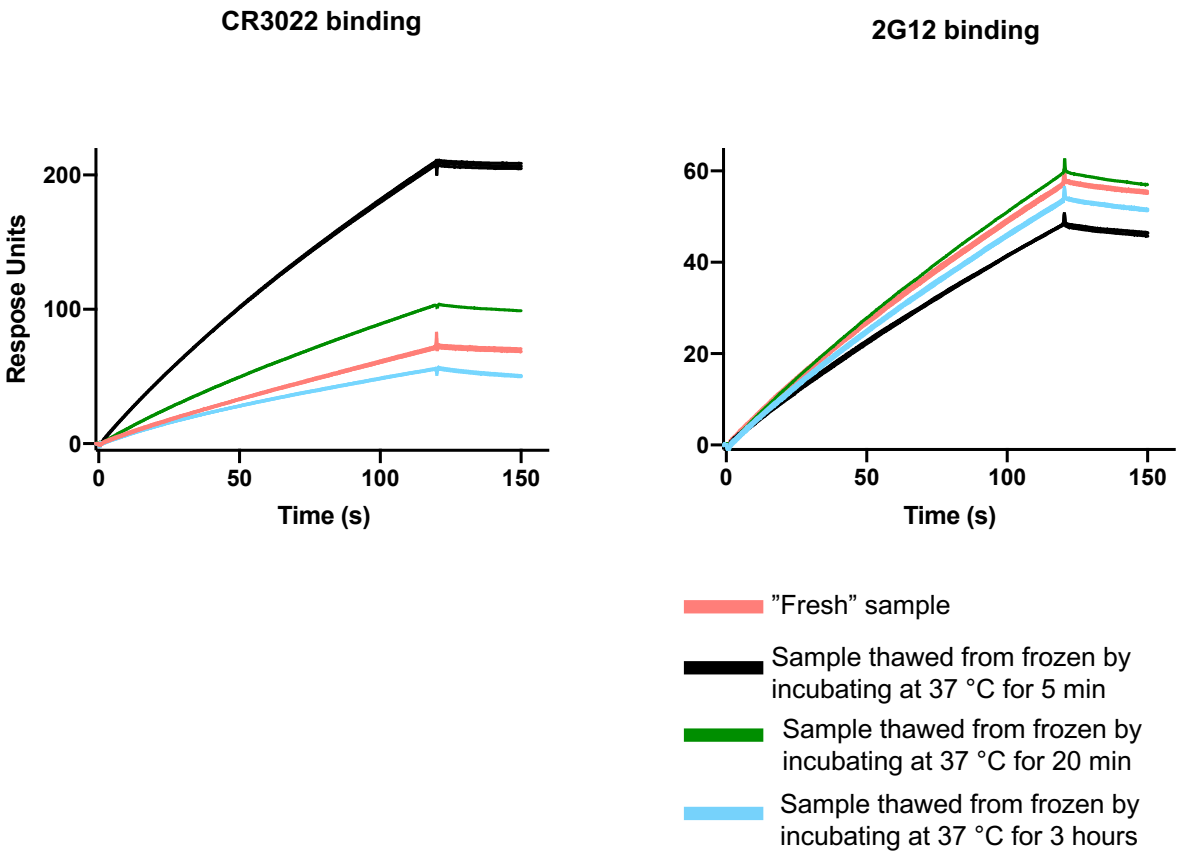

Supplementary Figure 3. CR3022 and 2G12 binding to freshly purified spike and spike that has been flash frozen then thawed. Antibody CR3022 IgG (left) and 2G12 IgG (right) binding to spike that was either freshly purified or flash-frozen in liquid N2, then thawed by incubating at 37 °C for different periods of time.

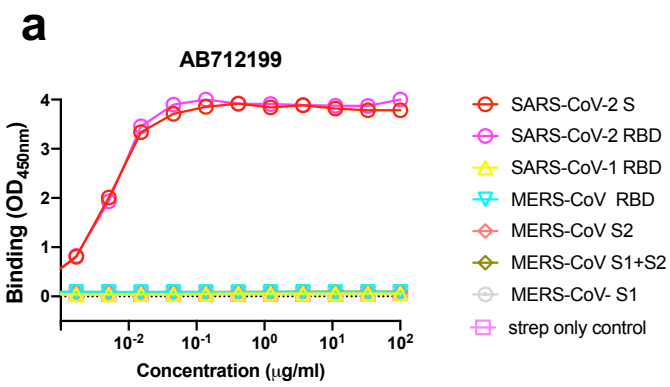

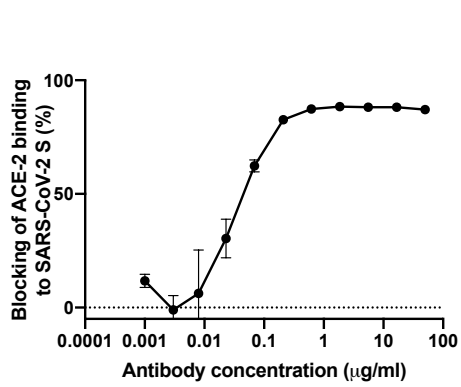

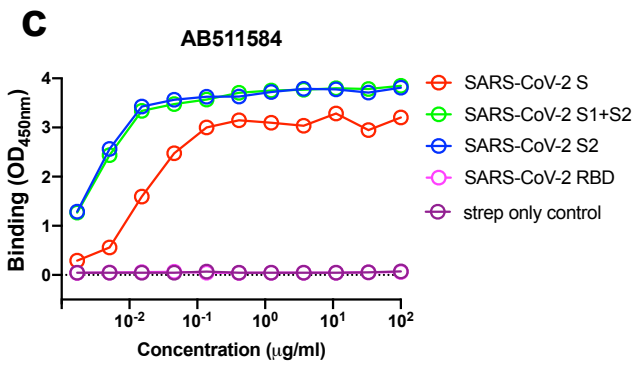

d

	SARS-CoV-2 Spike/2p	SARS-CoV-2 RBD	SARS-CoV-2 S2
AB511584	11.59	0	16.11
AB712199	16.705	17.048	0

Supplementary Figure 4. Characterization antibodies isolated from COVID-19 convalescent donors by ELISA (**a**) Epitope mapping of antibody AB712199 shows that the antibody binds the SARS-CoV-2 RBD region, (**b**) Blocking of ACE-2 binding to SARS-CoV-2 S ectodomain by AB712199, **(c)** Epitope mapping of antibody AB511584 shows that the antibody binds the SARS-CoV-2 S2 region **(d)** Summary of epitope mapping from ELISA showing log of the area under the curves.

a

	Microneutralization assay	Pseudovirus assay		PRNT		
	Geometric Mean Effective conc. (µg/ml)	IC50 (µg/ml)	IC80 (µg/ml)	IC50 (µg/ml)	IC80 (µg/ml)	IC90 (µg/ml)
Ab511584	>100	NA	NA	NA	NA	NA
Ab712199	0.55	0.012	0.11	0.316	0.120	0.863

b

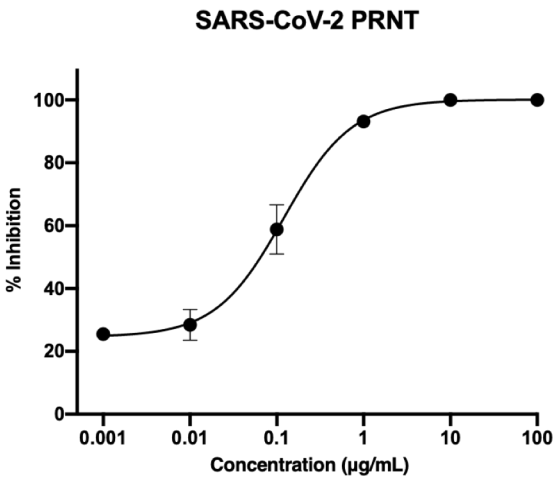

c

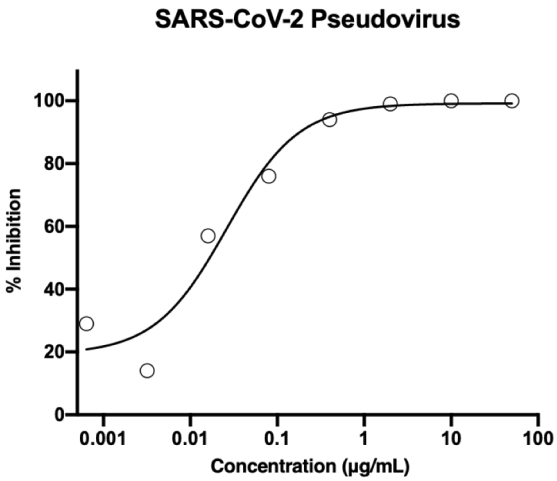

Supplementary Figure 5. Characterization antibodies isolated from COVID-19 convalescent donors in neutralization assays. (**a**) Summary of neutralization profiles of antibodies AB511584 and AB712199 by three different assays. (**b**) Neutralization of SASR-CoV-2 by AB712199 measured using plaque reduction neutralization test. **(c)** Neutralization of SASR-CoV-2 by AB712199 measured using a pseudovirus assay.